QUANTUM WELL INTERMIXING IN InGaAsP/InP LASERS USING LT-InP

QUANTUM WELL INTERMIXING IN InGaAsP/InP LASER STRUCTURES USING LOW TEMPERATURE GROWN InP

By

BROOKE E. GORDON, B.Eng

A Thesis

Submitted to the School of Graduate Studies

in Partial Fulfilment of the Requirements

for the Degree

Master of Applied Science

McMaster University

MASTER OF APPLIED SCIENCE (2002) McMaster University
(Engineering Physics) Hamilton, Ontario

TITLE: Quantum Well Intermixing in InGaAsP/InP Laser Structures Using Low -Temperature Grown InP

AUTHOR: Brooke E. Gordon

SUPERVISOR: Professor D. A. Thompson

NUMBER OF PAGES: x , 86

Abstract

This thesis presents quantum well intermixing in InGaAsP/InP quantum well laser structures using a low temperature grown InP (LT-InP) cap. The thermal response of the underlying semiconductor material was examined as a function of rapid thermal anneal temperature and time and is also studied with respect to structure thickness, surface composition (InGaAs or InP), choice of p- or n-type InP substrate and doping within the structure, and changes in growth temperature of the active region. It was found that structures with Be-doped cladding exhibit large enhanced intermixing through the possible dissociation of a grown-in defect complex. It was also found that a process, with an onset of ~690°C, becomes the dominant mechanism for intermixing in both full and partial laser structures at temperatures ≥750°C when the samples are annealed for 60 sec. It is proposed that this blueshift is the combination of another defect complex that dissociates at anneal temperatures ≥750°C to produce a fast diffusing defect that can enhance intermixing within <8 sec, and also group V vacancy diffusion that originates from the desorption of group V species from the samples' surface at high anneal temperatures and long times.

Intermixing was also studied as a function of the growth parameters of the LT-InP caps grown by GSMBE. It is shown that at temperatures below congruent sublimation for InP (360°C), P_{In} antisite defects are incorporated as a result of

non-stoichiometric growth. These defects are incorporated with decreasing growth temperature and also with increasing phosphine flow. The results will show that the rate of intermixing increases with increasing defect incorporation, and that the intermixing is not exhibited in samples with the LT-InP cap removed prior to annealing. Furthermore, the intermixing is seen to occur for anneal temperatures >640°C. Therefore, it is suggested that at this temperature there is sufficient thermal energy for the P_{In} antisite to dissociate into a P interstitial and In vacancy. The P interstitials are highly mobile in InP and subsequently diffuse rapidly to produce large blueshifts within <15 sec.

Acknowledgements

Many researchers have made contributions to this project. In particular I would like to thank Dr. Thompson for the opportunity to study, Brad Robinson for his infinite wisdom, and Peter Jonasson for keeping the coffee hot. I would also like to thank Andy Duft and Alexandra Perović for the AFM and TEM preparation and analysis, Alex Lee and J.F. Hazel for all their help, guidance and training, and J. Dallaire for the collection of data that summer. Most important, these years would not have been possible without the endless support of my family and friends. I would like to extend special appreciation to my parents, my darling sisters, and Nana.

Table of Contents

List of Figures

List of Tables

Chapter 1

Introduction to Quantum Well Intermixing

In 1969, Stewart Miller published a paper on integrated optics. He proposed a miniature form of laser beam circuitry formed by photolithography on a single substrate [1]. Although the original proposal was for the use of a glass substrate to guide the laser output, developments in semiconductor devices have further inspired a multitude of possibilities. Integrated semiconductor devices are known as photonic integrated circuits (PICS) or optoelectronic integrated circuits (OEICS). The goal is to tailor the band gap and refractive index in specific regions of the wafer to allow for the fabrication of multiple devices on a single crystal substrate. This can be done physically through etching and regrowth processes, or spatially in quantum well (QW) structures by various techniques that can induce quantum well intermixing (QWI).

Fabrication of an integrated device is a complicated, multi-step process. The conventional method of varying the band gap is by selective etching and regrowth of the semiconductor layers with different compositions. This process involves masking the epitaxial surface of the device using photolithography techniques to protect desired regions, and then etching down through the layers of upper cladding material and the active region. Care must be taken to ensure the etch reaches the appropriate depth and undercutting is prevented. The

sample must then be thoroughly cleaned before regrowth of the new active region [2]. With identical material composition in the upper cladding of the preserved and regrowth areas, a constant optical waveguide propagation coefficient is maintained across the wafer [3].

Another possibility for achieving different active and passive regions is by varying the depth of the active region across the wafer during the initial growth through the use of a patterned dielectric mask. This method of growth typically requires the use of metal-organic chemical vapour deposition (MOCVD) or metal-organic molecular beam epitaxy (MOMBE). In these systems, the atoms will have preferential growth in the dielectric windows, where the underlying semiconductor crystal is exposed. However, adsorption and surface migration of the growth species may take place across the mask so the growth rate, thickness uniformity and composition uniformity will depend on the thickness of the mask and dimensions of the windows [3]. Both these techniques also have significant potential for contamination at the surface from photolithography and etching, which could affect the quality of the epitaxial layers, resulting in a reduced performance and yield. These methods have been used to fabricate a variety of photonic components.

Quantum Well Intermixing

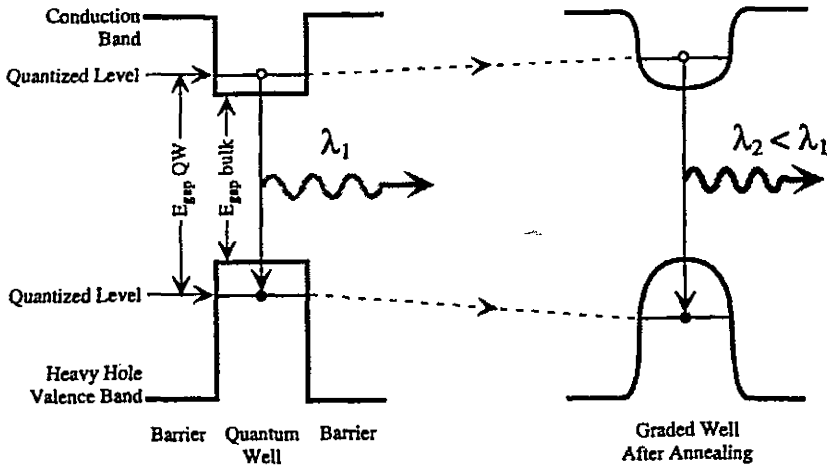

Figure 1.1 Change in the QW profile as a result of annealing[1].

Quantum well intermixing (QWI) is a technique that modifies the as grown composition and dimensions of the quantum wells and adjacent barriers in selected regions through spatially defined atomic interdiffusion within the structure. In III-V semiconductor structures, the interdiffusion process between atoms in the quantum wells and adjacent barriers involves mobile point defects, typically vacancies and interstitials. These defects mediate the diffusion of column III atoms and/or column V atoms [4, 5]. The profile of the QW is expected to change from a square well to a graded profile as shown in Figure 1.1. This leads to a variation in the well width and depth, and hence a reduction in quantum confinement [6]. The result is a change in the transition energy of the

[1] adapted from [12]

well and a corresponding shift in the emission wavelength towards shorter wavelengths [7], thus an alternate name to QWI is blueshifting.

In addition, modifications to the band gap will alter the absorption coefficient and the index of refraction via the Kramers-Krönig relations, which can alter the guiding properties of the structure [8]. Devices such as low-loss optical waveguides, modulators, lasers, and detectors have been fabricated using QWI on a single wafer.

There are various techniques available for enhancing QWI. These include impurity induced disordering (IID) [3], impurity free vacancy disordering (IFVD) [7, 9, 10, 11], laser induced disordering (LID) [3, 22], photoabsorption induced disordering (PAID) [3, 23] and employing epitaxial layers that promote intermixing [6, 12, 13, 14].

Impurity Induced Diffusion

In the case of IID, impurities are introduced into the crystal by diffusion from the surface or by ion-implantation. A thick dielectric mask is used to spatially restrict the impurities to desired regions within the semiconductor structure [15]. For ion-implantation, the energy of the ions and the thickness of the mask can be used to control the concentration and depth of the impurities implanted in the crystal. Zn (p-type) and Si (n-type) have been shown to be effective impurities for intermixing in GaAs/AlGaAs systems [3]. However, the introduction of such active dopants will cause problems in achieving electric isolation between integrated devices and could increase free carrier absorption of propagating light.

The use of neutral dopants, such as F and B, has been used by Marsh [7], however these species may still introduce changes to resistivity and non-radiative traps. Furthermore, the use of ion implantation to introduce the impurities is not appropriate for lasers and modulators due to residual damage to the crystal lattice from the energetic ions that cannot be completely removed by annealing [3].

Impurity Free Vacancy Disordering

IFVD is a promising technique in GaAs/AlGaAs systems because it can preserve high crystal quality, maintain low optical propagation losses, and not introduce unwanted dopants. As an extension of ion implantation, host atoms (In, Ga, As, P) may be implanted in InP and/or GaAs systems to limit the effects of unwanted doping and atomic interactions [9, 10]. The implanted atoms introduce a variety of crystal defects within the structure, which enhance self-diffusion of the host atoms upon anneal. Again, defects may remain in the form of residual crystal damage, which may act as non-radiative centres after annealing, altering the optical properties of the crystal.

In its most common form, IFVD refers to a sample encapsulated with a dielectric layer followed by annealing at elevated temperatures. The semiconductor material will intermix if point defects are created at the interface of the semiconductor surface with the dielectric cap [3]. Layers of SiO_2, $Si_xO_yN_z$ and phosphorus doped SiO_2 (SiO:P) are a few examples of dielectrics used to promote intermixing in GaAs or InP systems [11, 16, 17].

Ga is known to be soluble in SiO_2 at high temperatures. For the GaAs/AlGaAs and GaAs/InGaAs systems, Ga atoms from the underlying crystal in contact with the SiO_2 cap migrate into the cap layer, creating a non-equilibrium concentration of Ga vacancies (V_{Ga}) in the crystal [11]. During the anneal these group III vacancies diffuse deep into the structure and enhance interdiffusion on the group III sub-lattice. In the GaAs system the amount of QWI can be altered by varying the thickness of the dielectric material. Thicker encapsulation allows for a greater concentration of dissolved Ga, therefore the concentration of V_{Ga} will increase with the thickness of the dielectric. In contrast to GaAs based materials, studies related to encapsulation of InP based systems with an InGaAs surface layer have shown essentially no dependence on dielectric thickness [16, 18].

In the InP based systems intermixing allows for interdiffusion between the group V atoms (As and P). Rao et al. [11] used SiO:P to study interdiffusion on the group V sub-lattice. The presence of P in the SiO_2 enhanced the blueshift compared to samples encapsulated with undoped SiO_2. The blueshift was found to be proportional to the concentration of P in the encapsulation layer. It was proposed that the P diffuses into the underlying crystal in the form of interstitials, which enhances intermixing on the group V sub-lattice. Further evidence of interstitials as the mechanism for group V interdiffusion has also been presented in literature [14, 16, 19, 20].

One of the essential problems with dielectric encapsulation is the wide range of deposition techniques for the dielectric cap layer, which makes results

quite variable [21]. Furthermore, some deposition techniques may cause surface contamination and damage, and interface strain. These can affect the intermixing process and the presence of native oxides on the semiconductor surface will create further variability [3].

Laser Induced Disordering

LID refers to two methods of intermixing. The first uses a high-power CW laser that is used to generate carriers in the active region. This causes localised heating in the active region that promotes interdiffusion [16]. This technique is impurity-free and using a small beam spot, can induce intermixing locally without the use of a mask. However, the area selectivity is broadened due to the thermal conductivity of the sample [16]. Unfortunately, because this method of LID requires high power densities to melt the material, there is complete intermixing of the wells and barriers such that partial intermixing is not possible. Furthermore, the final structure may result in an undesirable redistribution of dopants [3].

The second method uses a pulsed laser to create uneven heating across the sample surface such that defects are created as a result of thermal shock. The sample is then annealed such that the surface defects diffuse to enhance QWI [3].

Photoabsorption Induced Disordering

An alternative to LID is PAID. This technique exploits the thermal properties of III-V QW structures. It is also impurity free, requires considerably reduced power density than other CW laser techniques, and is layer composition selective. The process depends on the band-gap of different layers within the structure. A wavelength is chosen for irradiation such that band to band absorption occurs only in the wells and barriers, generating heat and subsequent diffusion in the active region. This technique is not restricted to near-surface active regions; however, the outer layers must be transparent at the irradiation wavelength [3].

The surface of the sample can withstand damage if the temperature on the surface is accurately known as a function of laser beam power. However, the power is dependant on experimental parameters such as focusing, sample mounting, and ambient conditions such as humidity and dust on the surface of the sample [22]. This may lead to surface damage or non-reproducible results. Furthermore, the spatial selectivity of the laser beam is limited due to the Gaussian profile, resulting in non-uniform heating across the intermixing region. As with LID, the localised heating is further affected by the thermal conductivity of the material system [23].

Alternative Methods

The final method presented in this work is the use of epitaxial layers with grown-in native defects [4, 14]. At temperatures significantly below the normal growth temperature, III-V materials are found to be non-stoichiometric, containing a high concentration of intrinsic defects. It has been shown that low temperature grown GaAs (LT-GaAs) epitaxial layers can be used as an efficient source of surface defects to enhance QWI using LID and IFVD techniques [6, 22].

The III-V material system commonly used for telecommunication device applications is InGaAsP/InP. The results to be discussed in this report will demonstrate the effectiveness of low temperature grown InP (LT-InP) on QWI and attempt to describe the mechanism by which the LT-InP induces QWI.

Chapter 2

LT-GaAs

The desire for semi-insulating GaAs sparked an interest in its growth at low temperatures. The stoichiometry of GaAs depends on both the growth temperature and V:III ratio such that As anti-sites (As_{Ga}) and V_{Ga} are formed, and excess As is incorporated at low temperatures [6]. Post-anneal characteristics of LT-GaAs reveal a highly resistive layer that may be a result of the large concentration of native defects. As a consequence, this material has many applications for epitaxial processing, such as device isolation and current confinement [24, 25].

The As_{Ga} defect, also known as the EL2 centre, has been well characterised by electron paramagnetic resonance (EPR) when in its charged state, As_{Ga}^{+}. It has been shown that the concentration of As_{Ga} increases dramatically as the growth temperature is reduced [26, 27]. This is consistent with the findings of excess As incorporated at lower growth temperatures. It was also found [28] that V_{Ga} are incorporated in LT-GaAs grown by MBE at temperatures below 300°C.

A LT-GaAs layer will be strained due to the different bonding lengths of As-As compared to Ga-As and the strain varies with the amount of excess As incorporated in the layer [24, 29]. This will lead to a critical thickness for the

growth of a dislocation free LT-GaAs layer. Below the critical thickness these low temperature grown layers maintain high crystalline quality, allowing the native defect concentration to be exploited as a means of controlling the properties of the as grown material. Similar characteristics have also been reported for LT-AlGaAs and LT-AlInAs [25, 27].

Precipitates

The excess As in LT-GaAs has been found to form into spherical As-precipitates after annealing, resulting in strain relaxation [30]. These semi-metallic precipitates create a depletion region that can be modelled as Schottky barriers. If the space charge regions overlap, a completely depleted layer is formed that results in high resistivity, $>10^6$ Ω-cm [29, 30]. This high resistivity is only demonstrated after annealing, requiring defect migration in order to form the precipitates.

Quantum Well Intermixing using LT-GaAs

LT-GaAs has been used to enhance QWI in AlGaAs/GaAs and InGaAs/GaAs systems. The self-diffusion rate of atoms on the group III sub-lattice depends on the concentration of non-equilibrium defects in the crystal and also on compositional changes within the structure [32]. It was proposed [6, 31] that LT-GaAs enhance QWI via the point defects that result from non-stoichiometric growths. V_{Ga} has a high diffusion coefficient in GaAs and is expected to be the dominant defect that diffuses on the group III sub-lattice [6].

By the same premise as IFVD, an epitaxial layer of LT-GaAs provides a significant concentration of V_{Ga} that can diffuse as point defects to enhance QWI.

Previous results [4] showed that growth temperatures >250°C were required to maintain good quality GaAs grown by MBE, which will be discussed in further detail with regards to LT-InP. The study also showed that lowering the growth temperature of the quantum wells below 350°C results in enhanced intermixing of Al-Ga when the sample is subsequently annealed. This is a result of the LT-AlGaAs/GaAs material in the active region becoming more non-stoichiometric with decreasing growth temperature where a higher concentration of defects leads to a greater degree of intermixing for the same annealing conditions. Furthermore, the PL peak energy of the LT-AlGaAs/GaAs QW structure, which is used to measure the degree of intermixing, was found to increase non-linearly with both anneal time and temperature. Significant compositional changes (43.5nm) took place rapidly within the first 15 sec when the sample was annealed at 900°C, subsequently followed by a slow increase with time. This was attributed to the large diffusion coefficient of the V_{Ga} and the rate of change of the Al gradient between the quantum wells and adjacent barriers [4].

The composition of quantum wells and barriers can be grown such that tracking the Al composition in an AlGaAs/GaAs structure, or similarly the In concentration in InGaAs/GaAs, is an effective method of measuring the amount of disordering. Samples with a LT-GaAs cap layer were annealed at temperatures ranging between 750 and 900°C [6,31]. It was found that Al

diffused into the QW's and the reduced rate of intermixing with time was attributed to the non-linear time dependent Al gradient across the wells and barriers that was mediated by Al-Ga interdiffusion via V_{Ga}. The results revealed that the post-anneal composition of Al was almost uniform across the wells and barriers at sufficiently high temperatures and long times. This was in contrast to samples grown without a LT-GaAs cap layer, which had essentially no shift in the PL peak wavelength when annealed under similar conditions. The experiment was repeated using InGaAs/GaAs structures with a LT-GaAs cap layer to show that after a 1 hour anneal at 800°C there was strain relaxation in the active region and the In content was also uniform between the wells and barriers. This indicates complete intermixing between the wells and barriers such that the active region is comparable to an averaged bulk composition. Calculations were used to demonstrate that the interdiffusion coefficient of In-Ga was 1-2 times greater than for Al-Ga. The different coefficients were attributed to the weaker In-As bonds, indicating that the InGaAs/GaAs system is more easily disordered [33].

LT-InP

There have been some differences in the properties of LT-InP reported by various groups. These arise from the difficulty in accurately measuring the substrate temperature during MBE growth and uncertainties in the beam equivalent pressure of the P_2 flux. Therefore an element of variability exists when comparing results derived from different groups [29]. However, general trends

can be established with respect to the excess P incorporation found in epitaxial layers grown at low temperatures.

Several groups [25, 26, 27, 34, 35] began a study of LT-InP with the intent of creating intrinsically doped semi-insulating InP, analogous to the behaviour of LT-GaAs. This would have considerable advantages over the use of conventional Fe-doped InP because this dopant has low thermal stability, which leads to anisotropic electrical activity and dopant interactions in the presence of Zn [34].

Xie et al. [25] showed that 7 at% excess P was incorporated in samples grown at 200°C, Maracas et al. [29] measured 3 at% excess P in the LT-InP epitaxial layer grown at 240°C, and Docter et al. [24] found >5 at% excess P incorporated in the InP samples grown below 250°C. These results demonstrate that there is excess P incorporated in InP when the substrate temperature is reduced. Because of its smaller atomic size, it is expected that the excess P will be incorporated as interstitials (P_i), antisite defects (P_{In}), or complex defects, creating a non-stoichiometric material [34].

Precipitates

Analogous to LT-GaAs, the incorporation of P on In sites will result in tensile strain in the LT-InP layer due to the large difference in atomic size of P compared to In. A change in the lattice constant and the development of strain in the as grown LT-InP layer has been reported by several groups [24, 26, 36]. P precipitates have also been observed to form in LT-InP after annealing, indicating defect migration. Docter et al. [24] found that for a layer of LT-InP grown at

280°C, the presence of P precipitates following a 30 sec anneal at 600°C is accompanied by strain relaxation. There was further evidence of crystalline, P-rich precipitates in LT-InP grown at 240°C and annealed in-situ at 500°C for 10 min [27]. These P precipitates were larger in size than the As precipitates previously observed in annealed LT-GaAs but with less density [27, 30]. Our group has not observed P-precipitates at anneal temperatures used in this study.

Carriers & P_{In} Defect

In MBE grown InP there is direct evidence of an increase in the free electron concentration as the growth temperature is decreased [37, 38, 39, 40]. Even samples grown with heavy Be doping ($>10^{18}cm^{-3}$) were found [26, 37, 40] to be uncompensated, with n-type conduction in the LT-InP epitaxial layers. It has been suggested [37] that a native donor-like defect is incorporated during growth of this layer, which is related to the excess P incorporated in low temperature growths.

It was found [37] that the free electrons in LT-InP were localised in an energy level resonant with the conduction band as opposed to an isolated impurity or defect energy level. It was further shown that the first ionisation level of the double donor defect, P_{In} is resonant with the conduction band edge of InP and is therefore the probable source of these free electrons [38, 41]. Chen et al. [39] were able to correlate the free electron concentration with the P_{In}^{+}. They concluded that the n-type conductivity found in as grown LT-InP is a result of

intrinsic anti-site defects. This electrical property is in direct contrast to the high resistivity expected by analogy to that of LT-GaAs.

Quantum Well Intermixing using LT-InP

The epitaxial technique of growing low temperature semiconductor material is intrinsically clean and free of plasma damage that may occur with dielectric film deposition techniques [42]. It has been shown that a large blueshift in the measured PL peak energy (>64 nm) is observed [12] for LT-InP/InGaAs structures annealed for 30 sec at 750°C. It has been proposed [12, 13] that this large blueshift is a result of transient, grown-in defects that are highly mobile and diffuse predominantly on the group V sub-lattice. It is believed that P_i mediates QWI by the exchange mechanism [13, 14], a self-propagating diffusion mechanism where the interstitial atoms exchange with lattice atoms, which then become the mobile interstitial species (now As_i or P_i). We will propose that the as grown P_{In} defects dissociate during anneal resulting in a mobile P_i that enhances quantum well intermixing.

Structures comprised of LT-GaAs/InGaAs were annealed [6] at temperatures >800°C for times up to 120 min, which resulted in a blueshift of the measured PL peak wavelength (>40 nm). This is smaller than the blueshift observed for LT-InP/InGaAs annealed for 30 sec at lower temperatures [12]. It has previously been proposed [6, 31] that the blueshift in GaAs-based systems is mediated by group III vacancies (V_{Ga}). However, the mobility of P_i at room temperature has been shown to be substantially greater than vacancies

occupying group III or V sub-lattices [43]. Therefore, InP-based structures will undergo intermixing at reduced anneal temperatures and times compared to GaAs material systems.

The results to be discussed in this report demonstrate QWI in InGaAsP/InP multi-quantum well lasers grown with and without LT-InP cap layers. The effect of the growth conditions of the cap layer, including substrate temperature and P_2 flux, on the degree of intermixing will be described.

Chapter 3

Growth Conditions of Samples

Samples were grown by gas source MBE (GSMBE) at a rate of 1μm/hr on S-doped (100) InP substrates. The group V flow rate was 4.0 sccm for InP and 5 sccm for the quaternary layers (InGaAsP). Each laser structure was grown at a temperature of 470°C as measured by a pyrometer (emissivity setting 0.4). A thermocouple placed behind the sample, between the sample and heater, read 517°C during growth. It was used to estimate the growth temperature for the LT-InP layers because the pyrometer is insensitive below 400°C [36].

All samples have a laser active region composed of three undoped, 1.1% compressively strained, 5nm thick InGaAsP QW's confined by InGaAsP barriers, lattice matched to InP. The two barriers between the QW's are 10nm thick and the outer surrounding barriers are 70nm thick. The group III composition of the wells and barriers is constant such that only the group V composition differs. This active region is surrounded by 80nm thick upper and lower guiding layers of 1.15μm wavelength quaternary material. InGaAs etch stops, 5 or 10nm thick, have been included above the upper cladding to facilitate etch-back for making the photoluminescence (PL) measurements. These layers are used as a standard active region for 1.55μm lasers grown at McMaster and have been

designed to optimise quantum confinement and optical propagation. Beryllium was used to achieve p-type doping within specified layers and Si was used to create donors. The following sections present the schematics of growths used for this study.

Growth structures used to study thermal effects

Sample 2645	Sample 2649, 2770
	100nm InP (undoped)
	200nm InGaAs (p+)
	1.3μm InP (p=1x10^{18} cm^{-3})
	200nm InP (p=5x10^{17} cm^{-3})
5nm λ=1.15μm InGaAs (p=5x10^{17} cm^{-3})	5nm λ=1.3μm InGaAs (p=5x10^{17} cm^{-3})
50nm InP (p=6x10^{17} cm^{-3})	40nm InP (6x10^{17} cm^{-3})
80nm λ=1.15μm InGaAsP (p=5x10^{17} cm^{-3})	80nm λ=1.15μm InGaAsP (p=5x10^{17} cm^{-3})
70nm λ=1.24μm InGaAsP (undoped)	70nm λ=1.24μm InGaAsP (undoped)
5nm QW $In_{0.76}Ga_{0.24}As_{0.85}P_{0.15}$ 10nm barrier $In_{0.76}Ga_{0.24}As_{0.52}P_{0.48}$ 5nm QW $In_{0.76}Ga_{0.24}As_{0.85}P_{0.15}$ 10nm barrier $In_{0.76}Ga_{0.24}As_{0.52}P_{0.48}$ 5nm QW $In_{0.76}Ga_{0.24}As_{0.85}P_{0.15}$	5nm QW $In_{0.76}Ga_{0.24}As_{0.85}P_{0.15}$ 10nm barrier $In_{0.76}Ga_{0.24}As_{0.52}P_{0.48}$ 5nm QW $In_{0.76}Ga_{0.24}As_{0.85}P_{0.15}$ 10nm barrier $In_{0.76}Ga_{0.24}As_{0.52}P_{0.48}$ 5nm QW $In_{0.76}Ga_{0.24}As_{0.85}P_{0.15}$
70nm λ=1.24μm InGaAsP (undoped)	70nm λ=1.24μm InGaAsP (undoped)
80nm λ=1.15μm InGaAsP (n=5x10^{17} cm^{-3})	80nm λ=1.15μm InGaAsP (n=5x10^{17} cm^{-3})
750nm InP buffer (n=1x10^{18} cm^{-3})	750nm InP buffer (n=1x10^{18} cm^{-3})
n+ InP substrate	n+ InP substrate

Figure 3.1 Schematic of laser structures used for the study of thermal blueshift. Sample 2645 is a partial laser structure. Samples 2649 and 2770 are full laser structures that differ by the growth temperature of the active region (470°C and 430°C respectively).

The three samples in Figure 3.1 were grown to study the blueshift of a partial laser compared to a full laser structure. These samples were grown without a LT-InP cap layer, therefore the QWI induced upon anneal is the result of grown-in defects within the structure. This is called the thermal blueshift. The compositions of quaternary layers are described simply by their bandgap

wavelength. The dopant type and concentration of each layer is also presented in Figure 3.1. Sample 2645 is a partial laser structure that has been terminated with 50nm of Be-doped InP and a 5nm thick Be-doped InGaAs cap. Sample 2649 is a full laser structure, where the 1.5µm thick, Be-doped InP upper cladding layer would be used for etching the ridge structure in a ridge waveguide laser. The whole growth of these two samples was performed at a temperature of 470°C, as read by the pyrometer. Sample 2770 is essentially identical to 2649 except that the active region was grown at a reduced temperature of 430°C. It is expected that as the growth temperature is decreased in the active region an increase in the concentration of grown-in defects will occur and their subsequent diffusion will enhance QWI upon anneal.

Structures with different substrate doping

Sample 2826	Sample 2827
200nm InGaAs (n=4x10^{18} cm^{-3})	200nm InGaAs (p=4x10^{18} cm^{-3})
1.3μm InP buffer (n=1x10^{18} cm^{-3})	1.3μm InP buffer (p=1x10^{18} cm^{-3})
150nm InP buffer (n=4x10^{17} cm^{-3})	150nm InP buffer (p=4x10^{17} cm^{-3})
5nm InGaAs etch stop (undoped)	5nm InGaAs etch stop (undoped)
100nm InP (n=4x10^{17} cm^{-3})	100nm InP (p=4x10^{17} cm^{-3})
80nm λ=1.15μm InGaAsP cladding (n=4x10^{17} cm^{-3})	80nm λ=1.15μm InGaAsP cladding (p=4x10^{17} cm^{-3})
70nm λ=1.24μm InGaAsP barrier (undoped)	70nm λ=1.24μm InGaAsP barrier (undoped)
5nm QW $In_{0.76}Ga_{0.24}As_{0.85}P_{0.15}$ 10nm barrier $In_{0.76}Ga_{0.24}As_{0.52}P_{0.48}$ 5nm QW $In_{0.76}Ga_{0.24}As_{0.85}P_{0.15}$ 10nm barrier $In_{0.76}Ga_{0.24}As_{0.52}P_{0.48}$ 5nm QW $In_{0.76}Ga_{0.24}As_{0.85}P_{0.15}$	5nm QW $In_{0.76}Ga_{0.24}As_{0.85}P_{0.15}$ 10nm barrier $In_{0.76}Ga_{0.24}As_{0.52}P_{0.48}$ 5nm QW $In_{0.76}Ga_{0.24}As_{0.85}P_{0.15}$ 10nm barrier $In_{0.76}Ga_{0.24}As_{0.52}P_{0.48}$ 5nm QW $In_{0.76}Ga_{0.24}As_{0.85}P_{0.15}$
70nm λ=1.24μm InGaAsP barrier (undoped)	70nm λ=1.24μm InGaAsP barrier (undoped)
80nm λ=1.15μm InGaAsP cladding (p=5x10^{17}cm^{-3})	80nm λ=1.15μm InGaAsP cladding (n=5x10^{17}cm^{-3})
750nm InP buffer (p=1x10^{18}cm^{-3})	750nm InP buffer (n=1x10^{18}cm^{-3})
p+ InP substrate	n+ InP substrate

Figure 3.2 Schematic of laser structures grown with mirrored doping profiles. Sample 2826 was grown on a p+ substrate and sample 2827 was grown on an n+ substrate.

The two structures in Figure 3.2 were grown at normal temperature to study the effect of substrate doping on QWI.[1] The samples were designed to have mirrored doping profiles using Si and Be for specified layers as before. Sample 2826 was grown on a p+ substrate that was doped with Zn to form an n-i-p structure and the n+ substrate of sample 2827 was doped with S, forming a p-i-n structure.

[1] Samples from these structures have been used independently in a previous report regarding SiO_2 encapsulation. Please refer to [12].

Growth Conditions for LT-InP caps

100nm LT-InP or NT-InP cap layer (undoped)
5 or 10nm InGaAs etch stop (undoped)
100nm or 2μm InP buffer (undoped)
5nm InGaAs etch stop (undoped)
25nm InP (undoped)
80nm λ=1.15μm InGaAsP cladding (undoped or $p=5x10^{17}$ cm^{-3})
70nm λ=1.24μm InGaAsP barrier (undoped)
5nm QW $In_{0.76}Ga_{0.24}As_{0.85}P_{0.15}$ 10nm barrier $In_{0.76}Ga_{0.24}As_{0.52}P_{0.48}$ 5nm QW $In_{0.76}Ga_{0.24}As_{0.85}P_{0.15}$ 10nm barrier $In_{0.76}Ga_{0.24}As_{0.52}P_{0.48}$ 5nm QW $In_{0.76}Ga_{0.24}As_{0.85}P_{0.15}$
70nm λ=1.24μm InGaAsP barrier (undoped)
80nm λ=1.15μm InGaAsP cladding ($n=5x10^{17}cm^{-3}$)
500 or 300nm InP buffer ($n=1x10^{18}cm^{-3}$)
n+ InP substrate

Figure 3.3 Schematic of partial laser structures for samples 3200 to 3714.

Sample Number	Growth Temperature of LT-InP cap [C]	Phosphine Flow used for LT-InP cap [sccm]	Initial Wavelength [nm]
3200	300	4.0	1571
3413	300	4.0	1568
3525	300	4.0	1581
3526	270	4.0	1582
3529	517	4.0	1580
3530	330	4.0	1581
3532	360	4.0	1579
3533	285	4.0	1573
3535	300	4.0	1575
3536	300	2.14	1577
3541	300	4.0	1580
3659	410	4.0	1567
3660	300	3.0	1570
3661	300	5.75	1564
3714	517	2.50	1589

Table 1 Summary of the growth criteria for the different cap layers of samples 3200 to 3714.

All samples in Figure 3.3 were used to study QWI and were terminated above the active region with undoped layers of InP (100nm), InGaAs (5nm) and capped with 100nm of either LT-InP or InP grown at normal temperature (NT-InP). A summary of the growth temperature, as measured by the thermocouple, and the group V flux used to grow the cap layer is presented in Table 1 along with the measured wavelength of the as-grown material for each sample.

Samples 3413, 3525 and 3535 were grown essentially identically to gain a better understanding of the repeatability of the overall QWI process. Alternative growth layers were incorporated in sample 3200, where the 80nm upper cladding was p-type doped ($p=5x10^{17}$ cm^{-3}) and in sample 3541 the undoped upper InP buffer layer was 2μm thick. These alternatives have been included in Figure 3.3.

Regrowth Conditions for Processing

200nm InGaAs ($p=1x10^{19}$ cm^{-3})
1.4μm InP buffer ($p=1x10^{18}$ cm^{-3})
150nm InP buffer ($p=3x10^{17}$ cm^{-3})
5nm InGaAsP etch stop ($p=3x10^{17}$ cm^{-3})
100nm InP ($p=3x10^{17}$ cm^{-3})
80nm λ=1.15μm InGaAsP cladding (undoped or $p=5x10^{17}$ cm^{-3})
70nm λ=1.24μm InGaAsP barrier (undoped)
5nm QW $In_{0.76}Ga_{0.24}As_{0.85}P_{0.15}$ 10nm barrier $In_{0.76}Ga_{0.24}As_{0.52}P_{0.48}$ 5nm QW $In_{0.76}Ga_{0.24}As_{0.85}P_{0.15}$ 10nm barrier $In_{0.76}Ga_{0.24}As_{0.52}P_{0.48}$ 5nm QW $In_{0.76}Ga_{0.24}As_{0.85}P_{0.15}$
70nm λ=1.24μm InGaAsP barrier (undoped)
80nm λ=1.15μm InGaAsP cladding ($n=5x10^{17}cm^{-3}$)
500 or 300nm InP buffer ($n=1x10^{18}cm^{-3}$)
n+ InP substrate

Figure 3.4 Schematic of the full laser structure derived from samples 3200 and 3413. The regrowth layers are outlined in bold.

Samples 3200 and 3413 were used in an etch and regrowth process to produce a full laser structure. After inducing QWI by annealing at 725°C for 30 sec each sample was etched back to the 80nm upper cladding layer. Prior to regrowth the sample surface was exposed to ozone for 20 min followed by an HF bath and de-ionised (DI) water rinse cycle. The regrowths were performed at normal growth temperature (470°C) and is outlined in bold in Figure 3.4. The layers of the final structure, from top down, have the following functions for device processing: the InGaAs cap is highly conductive allowing for an ohmic metal contact to be formed, the 1.4μm InP is used to form the ridge in ridge-waveguide lasers, and the 5nm InGaAsP layer is an etch stop used to define the ridge depth when wet chemical etching is used to fabricate the laser. The results and complications regarding these growths will be discussed in further detail in Chapter 7.

Chapter 4

Characterisation Techniques

Preparation

Samples used to study QWI were cleaved from the wafer into rectangular pieces approximately $2mm^2$. Regions near the edge of the wafer were discarded since composition and thickness variations occur in this region, which may lead to significant uncertainties in the results. All samples were annealed using Rapid Thermal Annealing (RTA) for various times and temperatures followed by photoluminescence (PL) measurements.

Rapid Thermal Anneal

The annealing took place under a flowing N_2 atmosphere in an AG Associates 610 Mini-Pulse RTA furnace. Samples were placed between pieces of InP and annealed in a covered carbon boat that contains a small inlet for the flowing N_2 gas. The pieces of InP acted as a proximity cap in order to protect the sample from the evaporation of phosphorus off the surface. This may affect the rate of intermixing due to the generation of surface defects, which could affect the radiative coupling into the surface and hence the temperature of the sample, and may also reduce the PL intensities [44]. Samples with LT-InP cap layers

were annealed in groups with a piece from either 3525 or 3535 to give a direct comparison of the blueshifts of samples under the same anneal conditions.

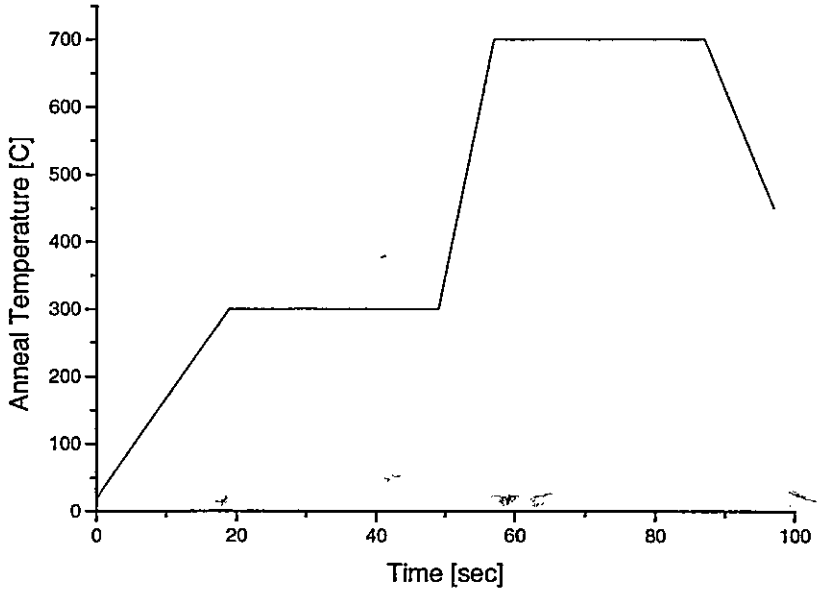

Figure 4.1 Typical anneal temperature-profile for an anneal at 700°C.

The temperature was controlled using a K-type thermocouple embedded in the carbon boat. The anneal temperature-time profile consisted of an initial increase to 300°C at a steady rate of 15°C/sec where it was held constant for 30 or 60 sec to ensure a stable temperature profile. This was followed by an increase at the maximum ramp speed, 50°C/sec to the desired temperature. A schematic of the temperature-time profile is shown in Figure 4.1. Anneal temperatures extend from 600-825°C for times ranging between 8-90 sec. The steady-state temperature stability is given by AG Associates as ±7°C [45]. After the anneal, the furnace was switched off and the cooling time with flowing N_2 gas took approximately 12 sec for the temperature to decrease by 100°C.

Photoluminescence

PL is the process of optically exciting carriers in the semiconductor material using an external light source and measuring the spontaneous emission spectrum emitted as the carriers recombine. A pump laser with an energy greater than the bandgap of the material is used to excite the carriers. For a direct bandgap material, the peak wavelength of the emission spectrum corresponds approximately to the bandgap energy of the crystal [46].

For PL measurements of the laser structures used in the thermal blueshift studies, light from an Ar^+ laser with an output of approximately 20mW was used as the excitation source. This was later replaced by a 10mW HeNe laser that was used for the QWI studies regarding LT-InP. In order to excite carriers in the QW active region it was necessary to remove all upper layers including both InGaAs etch stops. Each layer requires a different chemical solution followed by a rinse under running DI water. For InGaAs etch stop layers a solution of H_2SO_4:H_2O_2:DI (1:8:80) was used and HCl:H_3PO_4 (1:1) for InP. The etch time for the 100nm NT- and LT-InP cap varies with RTA treatment due to the formation of thin layers of quaternary material by interdiffusion into the underlying InGaAs layer. Although the InP buffer layer exhibits bubble formation on the surface during etching, samples were left in solution for >30 sec to ensure removal of the entire layer. Each InGaAs layer took approximately 45 sec to etch completely.

The PL spectrum was determined with a resolution better than 1nm using a monochromator with a pathlength of approximately 0.5m. The output signal was detected using an InGaAs photodiode and processed with a lock-in

amplifier. The wavelength was scanned over a range of 250nm at a rate of 1nm/step with a 990 msec dwell time. Two measurements were taken at each step and the detection phase was optimised at the beginning of data collection to maximize the signal strength.

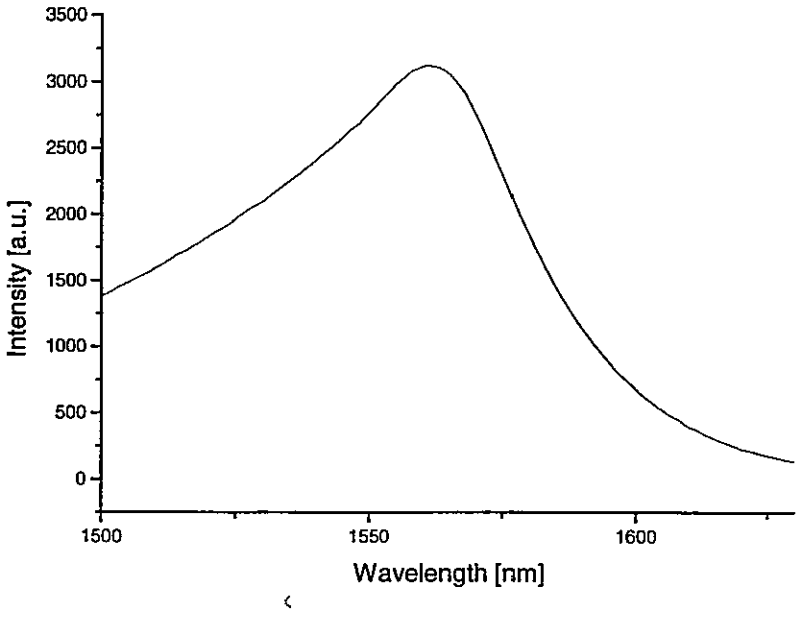

Figure 4.2 Typical PL spectrum of a sample taken at room temperature.

A typical PL spectrum determined at room temperature is shown in Figure 4.2. The degree of QWI was monitored by observing changes in the position of the peak wavelength in the PL spectra. As the intermixing occurs a blueshift in the peak wavelength is expected due to the modified QW shape, width and depth. The intensity of the peak is displayed in arbitrary units and the location of the peak wavelength is measured with a conservatively estimated error of ±1nm. The results throughout this work display the amount of blueshift calculated with respect to the as-grown peak wavelength of the samples shown in Table 1.

Reproducibility and an Estimate of Error

The following three samples were annealed at 725°C for 30 sec to gain a better understanding of the reproducibility associated with this method of QWI using LT-InP encapsulation in its entirety. The samples are partial structures with undoped upper guiding and etch stop layers, and a 100nm LT-InP cap grown at 300°C using excess P_2 flux. Samples 3525 and 3535 were clearly separated by 9 other growths, as indicated by their sample number, and were annealed both concurrently and consecutively. Sample 3413 was grown a few months earlier and annealed independently at that time.

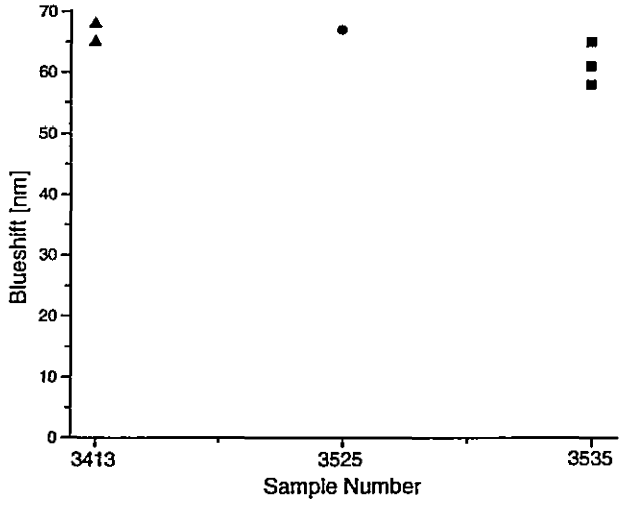

Figure 4.3 A scatter plot of the measured blueshift is shown for three samples to gain an estimate of the reproducibility with respect to the over all process.

The measured blueshift in Figure 4.3 is shown for multiple anneals of the three partial samples that are essentially identical in structure. It is clear that there is not a significant amount of scatter in the data. Sample 3525 had a

reproducible blueshift for all anneals, sample 3413 was reproducible within ±2nm, and sample 3535 was reproducible within ±3.5nm. The difference in the measured blueshift between the all the samples is ±5nm. This incorporates ±1nm from measurements of the PL peak, the RTA temperature control of ± 7°C and growth non-reproducibilities of the samples grown by GSMBE that arise from uncertainties in the substrate temperature and beam equivalent pressures. Error bars will not be included with the data to be presented since they are assumed to be ±5nm throughout this report.

Chapter 5

This chapter discusses the observed blueshift measured as a function of anneal temperature and time for samples that undergo RTA. This represents a measure of the quality of the as grown epitaxial structure and its stability against thermal annealing over the temperature range to be investigated. Since the self-diffusion coefficients are small [3, 47] any changes in the PL properties of the quantum wells can be associated with the diffusion of grown-in defects associated with the doped layers within the sample, or defects initially present in the substrate. These defects subsequently diffuse through the active region when the samples are annealed and enhance QWI by altering the size, shape, and composition of the quantum wells. As such, the sample structure, including doping, surface composition, and sample thickness are investigated with respect to the observed blueshift. The effect of surface degradation due to evaporation during annealing is analysed, as is the sensitivity of the active region to a reduction in the growth temperature by 40°C.

Observations Related to Thermal Blueshift

It has been shown previously [16, 42, 48, 49] that typically InP-based quantum well laser structures grown by either GSMBE or MOCVD exhibit a small blueshift in the measured PL peak energy after annealing. This is a result of interdiffusion of the host species within the active region, which is determined by

the composition gradient across the heterojunctions and also the presence of grown-in crystal defects that become mobile at the anneal temperature. These defects may arise from variations in the growth temperature, the beam equivalent pressures of the incident species and the doping concentration. Since high purity crystals have small diffusion coefficients for concentration driven diffusion at anneal temperatures well below the melting point [3, 47], a negligible change in the quantum well features, and hence a negligible blueshift in the PL emission, would be expected. Consequently, any blueshift that is observed in high purity crystals is expected to occur as a result of interdiffusion between the quantum well and adjacent barriers due to these grown-in defects and shall be referred to here as the thermal response of the material, or the thermal blueshift.

This report extends previous studies [16, 42, 48] to examine the thermal blueshift as a function of doping and sample structure using QW laser active regions. Full and partial laser structures underwent RTA treatments with the use of InP proximity caps for various times from 8-90 sec at anneal temperatures ranging from 650-825°C.

Thermal Response of the Quantum Well Active Region

The results shown in Figure 5.1 include three laser structures grown by GSMBE on n-type InP substrates at normal temperature (470°C as read by the pyrometer) as shown in Figure 3.3. Sample 3529 is a partial laser structure with undoped upper guiding and etch stop layers that is terminated with a 100nm thick NT-InP cap, and sample 3525 is a similarly grown partial structure but with a 100nm thick LT-InP cap grown at 300°C (as read by the thermocouple). Sample

3541 is a full laser structure with 2μm of undoped InP grown above the active region and also terminated with a 100nm thick LT-InP cap grown at 300°C. The LT-InP cap layer was removed from samples 3525 and 3541 prior to annealing by chemical wet etch as indicated by the "e" in order to examine the thermal response of the underlying semiconductor material. All samples were annealed at 725°C for various times to observe the thermal blueshift as a function of the different sample structures.

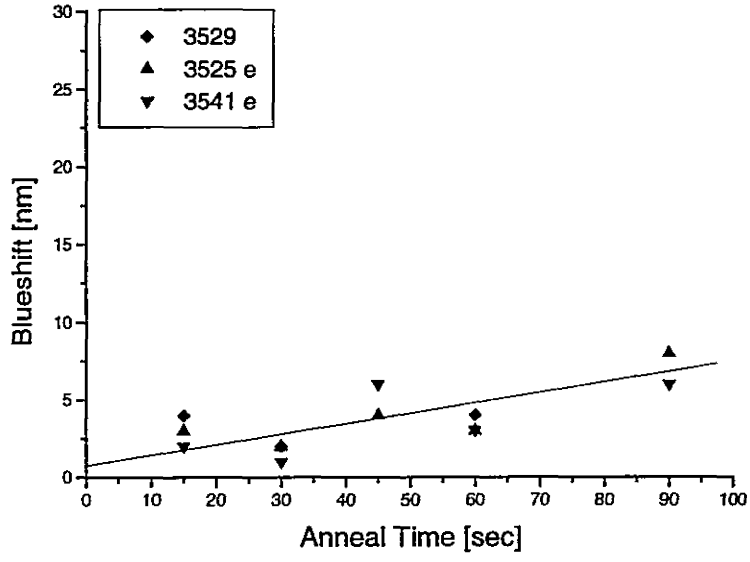

Figure 5.1 Measured blueshift due to thermal effects for a 725°C anneal as a function of time and shown with respect to sample structure.

It is seen in Figure 5.1 that there is <10nm of blueshift exhibited for all samples annealed up to 90 sec at 725°C and the blueshift is approximately zero at zero anneal time. The blueshifts of each sample are all in agreement within the expected error of ±5nm that arises from variations in the anneal temperature,

measurements of the PL peak energy and reproducibility of the growths as indicated in Chapter 4.

This study also uses annealed samples terminated with different surface layers (InP or InGaAs). Sample 3529, which is terminated with a 100nm NT-InP cap, has a structure similar to sample 3525; however, the 100nm LT-InP cap on sample 3525 was removed prior to annealing to expose the underlying layer of undoped InGaAs. Therefore, it can be concluded that the observed blueshift is independent of the surface layer. Furthermore, these results indicate that reducing the growth temperature to 300°C for growth of the LT-InP cap layer and then removing this cap layer by chemical etching prior to annealing does not contribute towards the observed QWI.

Sample 3541 is a full laser structure with an additional 2μm upper cladding layer of undoped InP above the active region which is not present in the partial laser structures. Because of its thickness this layer could potentially be a significant source of any grown-in defects that could induce additional QWI if they become mobile during the anneal and diffuse through the QW active region. Such grown-in defects may arise from variations in the substrate temperature and the incident flux of host species during growth, or from unwanted contamination doping. The abundant residual molecules found in McMaster's GSMBE are hydrogen from the gas source precursors, and those containing carbon and oxygen. The gas source precursors, arsine and phosphine, dissociate into H_2 and a group V dimer; however, any H_2 molecules present in the material either desorb during growth or out-diffuse during subsequent

annealing [50]. Carbon and oxygen containing molecules are present due to exposure of the growth chamber to air during routine maintenance. These may also be present, in small concentrations, in the sources, and can readily be desorbed from the many hot filaments and surfaces present in the vacuum chamber during growth. The concentrations of carbon and oxygen in laser structures grown by GSMBE have been previously measured within our group by SIMS [51]. It was found that a constant concentration ~$8x10^{15}$ cm^{-3} of carbon was present, and the incorporation of oxygen was ~$1.5x10^{17}$ cm^{-3} in the presence of Be doping, and ~$1.5x10^{16}$ cm^{-3} with no Be. However, these concentrations are considerably less than the intentional Be doping, which was measured to be ~$1.5x10^{18}$ cm^{-3}. Any contribution towards QWI from these contamination dopants in the lower cladding and active region is expected to be identical in both the full and partial samples. However, the blueshift of sample 3541, which has the additional 2μm of undoped InP grown above the active region, does not exhibit a consistently larger blueshift than the partial samples. These results indicate that this thick, undoped InP layer is not acting as a source of grown-in defects that could induce QWI.

Thermal Response of the Quantum Well Active Region Due to Anneal Time

Figures 5.2 (a-c) show the measured blueshift of three samples annealed for various times ranging between 8-60 sec at 700°C, 750°C and 800°C respectively. The samples were grown by GSMBE on n-type InP substrates as shown in Figure 3.1. Sample 2645 is a partial laser structure that has been terminated above the upper guiding layers with 50nm of Be-doped InP and 5nm of Be-doped InGaAs. The full laser structures, samples 2649 and 2770, have additional Be-doped layers consisting of 1.5μm of InP and 200nm of InGaAs above the upper guiding layers and are terminated with 100nm of undoped InP. The growths were performed at 470°C (as read by the pyrometer), except for sample 2770 where the active region was grown at 430°C. The objective was to determine if the annealing behaviour of the active region was sensitive to moderate changes in the growth temperature.

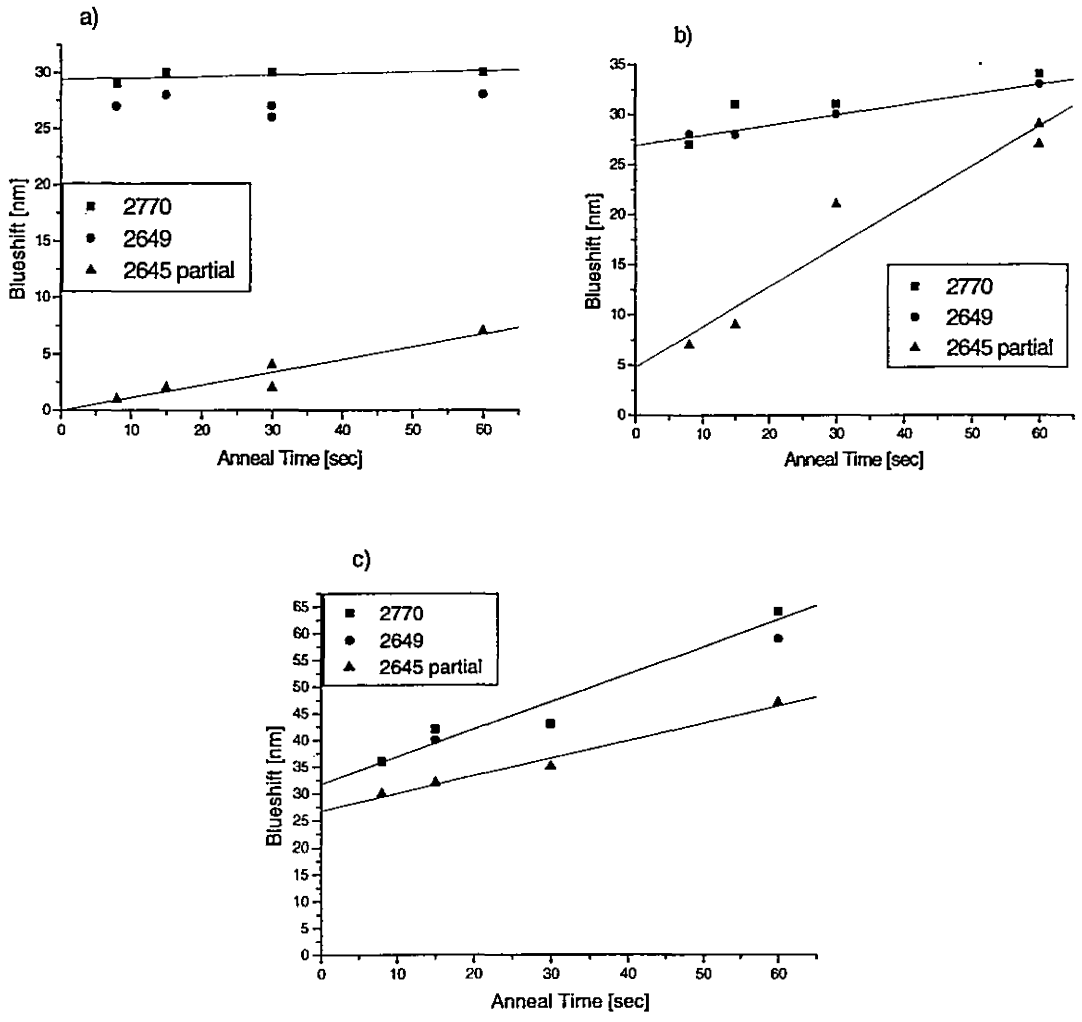

Figure 5.2 Measured blueshift due to the thermal response for (a) 700°C and (b) 750°C and (c) 800°C anneals as a function of time and shown with respect to sample structure.

From Figures 5.2 (a-c) it is observed that any changes between growths at 470°C and 430°C are the same within the experimental uncertainties of ±5nm. Since this temperature difference is well in excess of our ability to control the growth temperature, it is concluded that differences between the samples are not related to variations in the growth temperature of the active region.

Figures 5.2 (a-c) also show a comparison of the anneal properties of the partial and full laser structures annealed for times up to 60 sec at temperatures of 700°C, 750°C and 800°C. For the partial laser structures it is clear from Figure 5.2 (a) that sample 2645 exhibits a slow increase in blueshift with time that is consistent with the thermal blueshift presented in Figure 5.1. In Figure 5.2 (b) the blueshift for sample 2645 increases at a faster rate of 0.40 ± 0.06 nm/sec and appears to converge with the blueshift of the full laser structures after 60 sec. It is also noted that the blueshift extrapolates to ~5nm at zero anneal time, so a fast blueshift response of 7nm occurs within the first 8 sec of anneal. Furthermore, it is clear from Figure 5.2 (c) that the partial laser structure annealed at 800°C has an initial blueshift of 30nm that occurs within <8 sec and subsequently increases steadily with time at a rate of 0.32 ± 0.03 nm/sec. The blueshift for the 60 sec anneals at 750°C and 800°C are also consistent with previously published data of similar partial structures [16].

Both full laser structures (2946, 2770) in Figures 5.2 (a-c) exhibit a large blueshift that occurs within <8 sec of anneal. At 700°C, the blueshift is 27nm at 8 sec and remains approximately constant for anneal times up to 60 sec. Figure 5.2 (b) shows a similar initial blueshift but then increases approximately linearly at ~0.1nm/sec after 8 sec. The samples annealed at 800°C show a larger initial increase of 35nm followed by a linear increase of 0.5 ± 0.1nm/sec for times greater than 8 sec. The rate of intermixing was calculated by linear regression with a value of $R^2 = 0.99$ and the error is given relative to the line of best fit.

A previous study [48] of thermal blueshift used lattice matched InGaAs QW structures with InGaAsP barriers grown by MOCVD that were annealed in-situ for 2 hours at 750°C. After the anneal the QW had greater tensile strain than the as grown material and the barriers were found to be in compression. This lattice mismatch indicates a change in the composition of both the QW's and barriers. It was found that the rate of interdiffusion was equal within the same chemical group, however only the group V species had significant diffusion lengths. Therefore the observed thermal blueshift of their samples was due to the interdiffusion of group V species. The samples used in our study all have a constant group III composition throughout the wells and barriers such that any contribution to QWI that is observed must also be the result of interdiffusion of the group V species.

There are important observations to be made regarding the data in Figures 5.1 and 5.2. First, in Figures 5.2 (a-c) it is seen that the full lasers exhibit a large initial blueshift (>25nm) that occurs within <8 sec. These full lasers have a 1.5μm cladding layer of Be-doped InP grown above the active region compared to the partial structure. In contrast, it was previously shown in Figure 5.1 that a full laser structure with undoped InP upper cladding and InGaAs layers does not show this large blueshift occurring at the shortest anneal time. Instead, the blueshift extrapolates to approximately zero at zero anneal time and appears to increase slowly with time up to 90 sec. This suggests that specific defects are present in the Be-doped upper cladding that diffuse rapidly through the active region during annealing at temperatures below 700°C, resulting in enhanced

QWI that occurs for our shortest anneal time (8 sec). The fact that this effect is not present for the laser with undoped cladding suggests that these fast diffusing defects are related to the Be doping.

The initial blueshift for the full laser structures in Figures 5.2 (a-c) is essentially the same at 700°C and 750°C and only shows a small increase at 800°C. Also, the large blueshift that occurs in the full laser structures remains constant when annealed for up to 60 sec at 700°C. These observations suggest that a fixed concentration of migrating defects is responsible for this initial blueshift. This is consistent with the proposition that the initial rapid blueshift is associated with the Be-doped thick upper cladding layers. Also, the defect responsible for this initial QWI must have a low activation energy for migration below the anneal temperatures. One type of intrinsic defect that is mobile, even at room temperature is the P-interstitial [43], and this would cause interdiffusion on the group V sub-lattice through diffusion via the exchange method [13, 14]. Thus it is reasonable to speculate that some defects are grown into the Be-doped layers that involve a P-atom bound to a Be dopant. Then at some temperature above the growth temperature (470°C) but below 750°C this complex defect dissociates and produces P-interstitials, which then diffuse rapidly to cause the initial large blueshift.

The second observation regards the general behaviour of the partial laser structures for times >8 sec, which is a linear increase in blueshift with time. This rate of change increases from 700°C to 750°C but appears to be somewhat reduced at 800°C. During the higher temperature, longer time anneals some

samples showed visible signs of surface damage after removal from the RTA furnace. This was particularly evident for >30 sec anneals at 750°C and 800°C even though InP proximity caps were used and the anneals were carried out in a covered carbon boat that had been used many times before and had become saturated with phosphorus. The least damaged surfaces appeared frosted or opaque, instead of featureless and mirror-like. In the worst cases there was evidence of metallic In forming on the surfaces. This confirms that group V species are evaporating from the surface and this would be expected to leave behind group V vacancies that can diffuse into the sample and through the active region. A blueshift caused by group V vacancy diffusion has also been previously observed [3, 52] where the inter-diffusion of group V species between the wells and barriers was shown to be the result of group V desorption from the sample surface during the anneal.

For the 700°C and 750°C samples it seems reasonable to conclude that the change in blueshift with time of the partial laser structures is consistent with group V vacancy diffusion from a source at the surface of the samples. The same explanation would then be consistent with the time and temperature dependence of the blueshift of the full laser structures. However, the 800°C data shows a smaller rate of change than at 750°C for the partial laser and a larger rate of change for the full lasers. This may in some way be related to the fact that at 800°C the surface damage was much more severe than at 750°C.

The final observation to note is the fact that the partial laser structures annealed at 750°C and 800°C also show an initial rapid blueshift for time <8sec.

This is only small (7nm) at 750°C but becomes large (28nm) at 800°C. It appears that another fast diffusing defect is produced at temperatures ≥750°C which enhances QWI. We speculate that another defect complex is formed during growth, and this complex dissociates at ~750°C to also release a fast moving defect that is again likely to be a P interstitial. This complex defect in the partial lasers could originate from within the active region, the doped guiding layers surrounding the active region, or possibly the purchased substrate.

To summarise, there appear to be three processes that contribute towards the blueshift behaviour observed in Figures 5.2 (a-c). For the full laser structures there is a defect complex associated with the Be-doped upper cladding layer. These dissociate at anneal temperatures below 700°C to produce fast diffusing defects that produce a large blueshift within 8 sec. It appears that another defect complex is present in the partial samples that dissociates at ~750°C to produce a fast diffusing intrinsic defect that is also likely to be a P-interstitial. Finally, a source of defects that depends on both anneal time and temperature is present in the full and partial laser structures. The concentration of defects appears to increase rapidly with anneal temperature and subsequently results in a linear increase in the blueshift with anneal time. This enhanced QWI is expected to be the result of mobile defects originating from the evaporation of group V species from the sample surface. These results indicate that the use of proximity caps may not be adequate protection of the sample surface for prolonged anneals at temperatures >750°C.

Thermal Response of the Quantum Well Active Region Due to Anneal Temperature

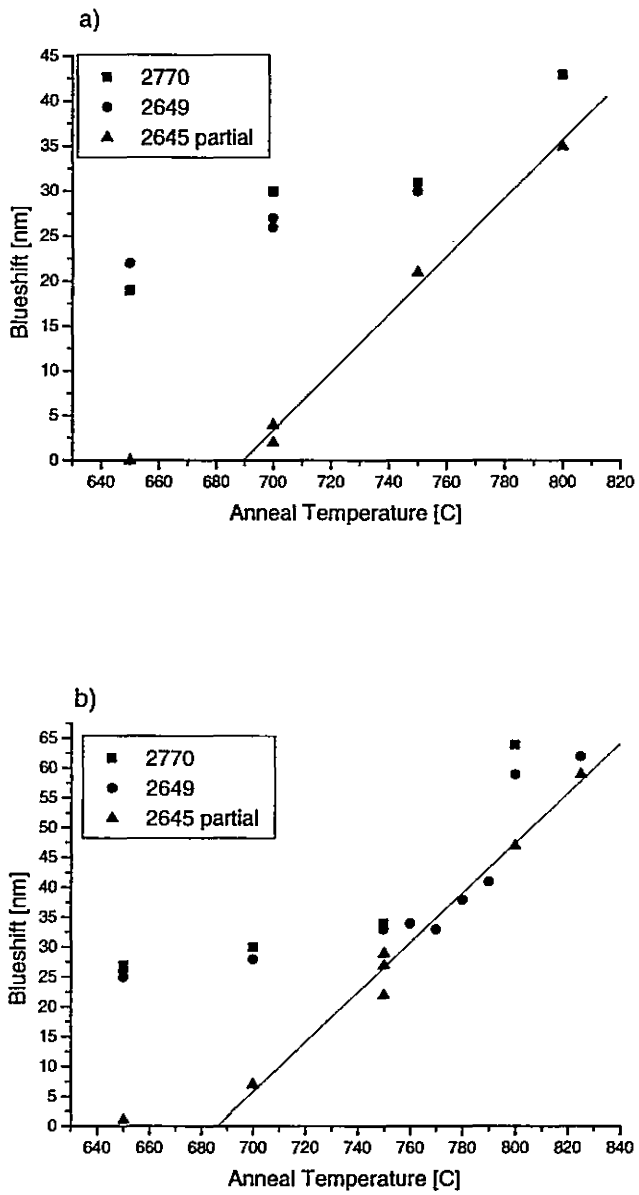

Figure 5.3 Measured blueshift due to thermal effects for (a) 30 sec and (b) 60 sec anneals as a function anneal temperature and shown with respect to sample structure.

The samples used for this study have been described in the previous section. All samples were annealed with InP proximity caps for 30 or 60 sec at temperatures ranging between 650-825°C.

In Figure 5.3 (a) the full laser structures (2649, 2770) exhibit ~20nm of blueshift when annealed for 30 sec at 650°C. This is followed by a steady increase in blueshift with anneal temperatures up to 800°C at a rate of 0.14 ± 0.02 nm/°C. In contrast, for the partial laser structure (2645) the blueshift increases linearly with anneal temperature at a rate of 0.25 ± 0.04 nm/°C, extrapolating back to an onset at ~690°C, as shown by the line. Furthermore, the measured blueshift of both full and partial samples appears to converge as the anneal temperature increases to 800°C. This is seen more clearly for the 60 sec anneals in Figure 5.3 (b) where the blueshift of the partial laser structure also increases linearly with anneal temperature at a rate of 0.4 ± 0.04 nm/°C. This data also extrapolates back to an onset at ~690°C. In contrast, the full laser structures annealed for 60 sec at 650°C have a measured blueshift >25nm and the blueshift increases slowly with anneal temperature up to 750°C. At anneal temperatures above 750°C, the blueshift of the full laser structures converges with the partial structure at a rate of 0.4 ± 0.04 nm/°C. The data at 800°C in Figure 5.3 (b) is anomalously high for the full laser structures. This may be related to non-reproducibility due to surface dissociation.

These results confirm the previously described processes contributing to the blueshift. First, the full structures exhibit similarly large blueshifts when annealed for both 30 sec and 60 sec at 650°C-750°C that is not exhibited by the

partial laser structure. This again suggests that defect complexes associated with the fixed Be doping would account for the fact that this component of blueshift is essentially independent of both anneal time and temperature.

In Figure 5.3 (b) the blueshift of the partial laser structures increases linearly with temperature and extrapolates to an onset at ~690°C. The second process that affects QWI is evident by the full laser structures, which initially have a slow increase in blueshift with anneal temperatures below 750°C. Subsequently, there is a greater rate of intermixing with anneal temperature that essentially converges with the blueshift of the partial laser structure. The results indicate that this second process, with the onset at ~690°C, is the dominant mechanism that causes intermixing in both the full and partial structures for anneal temperatures ≥750°C. It was previously noted that there was evidence of surface degradation for partial samples annealed at 750°C and 800°C due to the desorption of group V species from the sample surface at high anneal temperatures and long times. We would surmise that this dominant process is due to combination of group V vacancy diffusion originating from the sample surface, and also the dissociation of a defect complex at ~750°C, which produces a fast diffusing intrinsic defect that is likely a P-interstitial.

p Versus n Substrates

A comparison is made in Figure 5.4 between full lasers with mirrored doping to ascertain whether a p-i-n or n-i-p structure affected the thermal response. The n-type substrate was heavily doped with S and the p-type substrate with Zn. Doping of the cladding layers within the structures was achieved using Be (p-type) and Si (n-type) as shown in Figure 3.2.

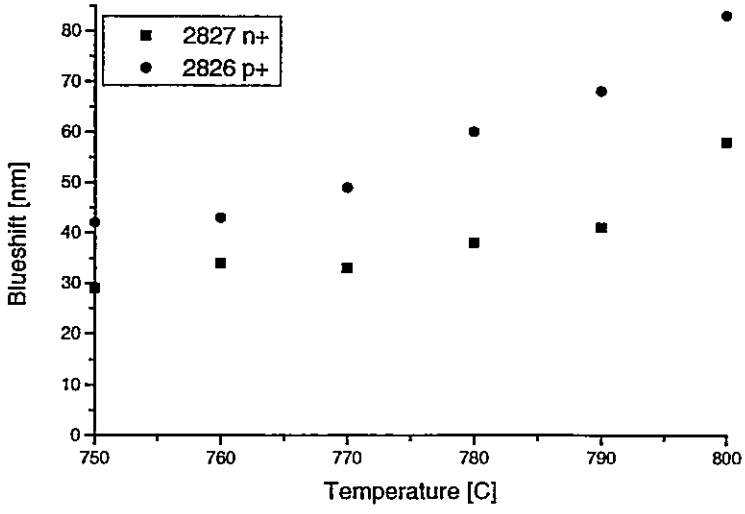

Figure 5.4 Blueshift versus anneal temperature for 60 sec anneals of partial laser structures grown on n and p substrates.

It is clear from Figure 5.4 that the blueshift increases with anneal temperature for both samples. The magnitude of the blueshift of sample 2827 is consistent with the previous results in Figure 5.3 (b) for a doped, full laser structure grown on an n-type substrate and annealed for 60 sec. Furthermore, it is clear that the laser structure grown on a p+ substrate has a consistently larger blueshift at all anneal temperatures.

The dopant used to create the p+ substrate is Zn, which has been shown to be an impurity that diffuses very rapidly on the group III sub-lattice and enhances QWI in GaAs/AlGaAs structures [3, 32]. Although some intermixing of the group V species may occur, it has been found that in InGaAsP/InP quantum well structures Zn also enhances interdiffusion predominantly on the group III sub-lattice [53]. Hence, Zn diffusion is not expected to contribute significantly to the QWI in our InP-based samples, which have identical group III composition throughout the wells and barriers.

Other evidence within our group [16, 54] has also shown that intermixing depends on the choice of doping in the cladding layers. Completely undoped structures grown on n-type substrates were found to exhibit less blueshift compared to structures with Be-doped upper guiding layers. The addition of Si doping in the guiding layers below the active region was found to further enhance QWI, and samples with both Si and Be-doped layers surrounding the active region exhibited the greatest blueshift [54]. Furthermore, internal fields created by the n-i-p or p-i-n junction of the laser structures may play a role in the interdiffusion process if the defects that cause the QWI are charged. However, these results are inconclusive as to the nature of the defects that causes intermixing.

It has been previously reported [55] that structures grown on InP substrates with high etch-pit densities will have less intermixing. It was proposed that substrate dislocations propagate into the epitaxial layers during growth and act as traps for mobile defects. The n-type and p-type substrates used in Figure

5.4 were purchased from a manufacturer who uses the same crystal pulling method with comparable etch-pit densities for each type of substrate. However, the concentration of point defects is not specified by the manufacturer, thus it is possible that the Zn-doped substrates may contain a greater concentration of point defects compared to the S-doped substrates, which may contribute towards the enhanced QWI.

Conclusions

In conclusion, reducing the growth temperature of the active region by up to 40°C has no significant impact on the amount of blueshift seen in full laser structures. Also, growth and subsequent removal of the LT-InP cap layer prior to annealing does not introduce defects into the underlying crystal structure that contribute to QWI.

The thermal blueshift that occurs as a result of annealing as grown laser structures depends on the doping within the structure. It was clearly seen that the n-i-p laser structure grown on a Zn-doped substrate exhibited a consistently larger blueshift than the p-i-n structures, which are grown on an S-doped substrate. Furthermore, the full laser structures grown on n-type substrates with Be-doped InP upper cladding and InGaAs layers exhibit an initial large blueshift that is not evident in a similar full structure with undoped layers. This large blueshift appears to be independent of anneal temperature at short times, suggesting that it is associated with the fixed Be doping. It is proposed that a Be-P defect complex dissociates at a temperature <700°C but above the growth

temperature (470°C), which produces a fast diffusing P-interstitial that enhances QWI.

The final observation is for anneal temperatures >750°C where it was observed that an initial rapid blueshift is exhibited within <8 sec by the partial lasers. This is likely the dissociation of another defect complex that produces a fast diffusing P-interstitial, which further enhances QWI. It was also shown that the use of RTA treatments at high temperatures and long times results in the evaporation of group V species from the sample surface, despite the use of InP proximity caps. This evaporation causes an enhanced blueshift that is expected to be the result of mobile group V vacancies originating from the sample surface. A process with an onset at ~690°C, as seen by the thermal response of the partial lasers, becomes the dominant source of QWI in both full and partial laser structures at temperatures >750°C for 60 sec RTA treatments. Therefore, this process is likely a combination of group V vacancy diffusion due to evaporation and also the dissociation of a complex defect. If the samples are to be used for device fabrication, surface damage may result in altered wet chemical etch rates and complications regarding MBE regrowth, therefore the use of anneal temperatures below 750°C is required to prevent surface degradation of the samples.

Chapter 6

This chapter discusses the enhanced QWI, as a function of anneal temperature and time, for samples terminated with a 100nm thick InP cap grown at various temperatures. This cap layer is shown to incorporate specific defects at low temperatures that can significantly enhance QWI when the sample is annealed. As such, the growth conditions of the LT-InP cap layer, including the growth temperature and P_2 flux, and sample thickness are investigated with respect to the observed QWI.

Observations Related to Low-Temperature InP

For samples grown by GSMBE, it is necessary to provide heat to the substrate in order to give the incident atoms sufficient kinetic energy to migrate on the surface. Subsequently, the atoms will bond into a normal lattice site, thus maintaining the lowest atomic energy configuration. As the growth temperature is reduced, a larger fraction of the incident atoms will become incorporated into non-normal lattice sites, resulting in non-stoichiometric layers.

For InP the congruent sublimation temperature is 360°C. Above this temperature P evaporates preferentially from the sample surface, thus an excess P_2 flux is required to maintain stoichiometric, single crystal growths. As the substrate temperature is reduced below 360°C, the use of excess P_2 flux along

with a reduction in the surface atom mobility will result in incorporated point defects, such as In vacancies, P interstitial atoms (P_i), and P antisites (P_{In}).

It has been reported [28, 56] that In vacancies are present in InP grown at temperatures below 300°C. However, the sample structures used in this work have a constant group III composition throughout the wells and barriers. Therefore, the diffusion of group III related defects are not expected to contribute towards any enhanced QWI. In the case of P_i, these have been shown to be highly mobile, even below room temperature [43] so at the growth temperature they are expected to rapidly diffuse out of the sample, or to various internal or external surfaces. Evidence was also presented in Chapter 2 that more P_{In} are incorporated in LT-InP as the growth temperature is decreased [37, 38, 39, 40]. Therefore, it is postulated that the dominant defects in the LT-InP cap layer, which contribute towards enhanced QWI in our samples, are P_{In} antisites.

It has been shown previously [12, 13, 14, 42] that laser structures with layers of LT-InP exhibit a large blueshift in the measured PL peak energy after annealing. These results indicate that LT-InP can be used to enhance QWI. This section extends these previous studies to examine the blueshift as a function of the growth parameters of the LT-InP cap layer, including substrate temperature and phosphine flow.

Effect of InP Growth Temperature on Intermixing

Throughout this section the pyrometer does not read below 400°C, as such, all measurements reported are thermocouple temperatures. Recall earlier that a normal growth at 470°C (as read by the pyrometer) results in a

thermocouple reading of "517°C". Henceforth, all thermocouple temperatures will be in quotation marks and it should be noted that the real growth temperature is lower. The partial laser samples used in Figure 6.1 were grown by GSMBE at normal temperature and terminated with a 100nm thick LT-InP cap grown with a fixed phosphine flow (4.0 sccm) at temperatures ranging between "270-517°C". All samples subsequently underwent RTA with the use of InP proximity caps for 30 sec anneals at temperatures ranging between 650-780°C.

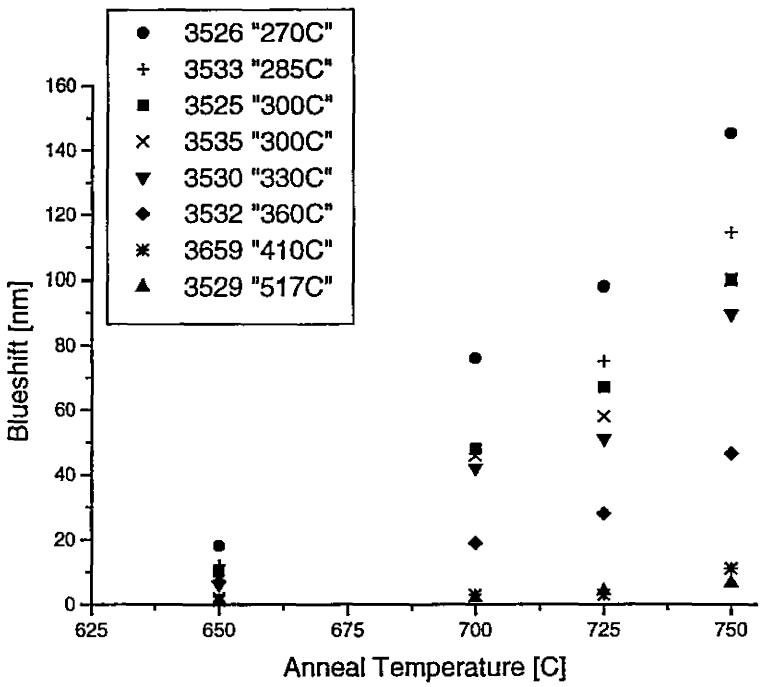

Figure 6.1 Measured blueshift as a function of anneal temperature for a 30 sec anneal and shown with respect to the growth temperature of the LT-InP cap.

The samples are identified in Figure 6.1 by their sample number and also by the growth temperature of the LT-InP cap for comparison of the measured blueshift with the growth conditions. Sample 3529 was grown at normal

temperature, and samples 3525 and 3535 are essentially identical structures terminated with LT-InP grown at "300°C". There is good agreement between the two "300°C" grown samples, which is the growth temperature used for LT-InP studies in previously published studies [14, 42]. It is clearly seen in Figure 6.1 that the measured blueshift increases steadily with anneal temperature and also with decreasing growth temperature of the LT-InP cap.

Partial laser structures with InP caps grown above "400°C" exhibit a small increase in blueshift for 30 sec anneals at temperatures above 700°C. These results are consistent with the thermal blueshift observed in Figure 5.1. At all temperatures below "400°C" a significantly enhanced blueshift is observed. Recall that these are thermocouple temperatures, which are higher than the actual growth temperature. As such, all growths carried out below "400°C" are actually below the congruent sublimation temperature (360°C) and, because of the excess P_2 flux, will incorporate point defects, which may diffuse through the active region upon annealing and enhance QWI. Therefore, the term LT-InP caps used in this study refers to samples terminated with 100nm of InP grown at temperatures below "400°C", which excludes partial laser structures 3529 and 3659 in Figure 6.1.

It has been shown [37, 38, 39, 40] that the incorporation of P_{In} antisites in LT-InP increases with decreasing growth temperature. Also, LT-InP is an n-type material that remains uncompensated when doped with Be ($>10^{18}$ cm^{-3}) [26, 37, 40]. Therefore, it is considered that the LT-InP cap contains a large concentration of P_{In} antisite point defects, which may dissociate into P-interstitials and In-

vacancies when sufficient anneal temperature is applied. From earlier electrical measurements on LT-InP grown at "300°C" it can be established that the concentration of the electrically active donors is ~$2x10^{18}$ cm^{-3} [36], which upon dissociation and diffusion would be capable of creating a significant effect on QWI. It has been shown that the diffusion of P-interstitials is greater than the diffusion of vacancies on either sub-lattice, even at room temperature [43]. Also, since the group III composition remains constant, it is expected that the resulting In vacancies will not contribute towards the observed QWI. Therefore, it is expected that the QWI is the result of fast diffusing P-interstitials and the exchange mechanism [13, 14].

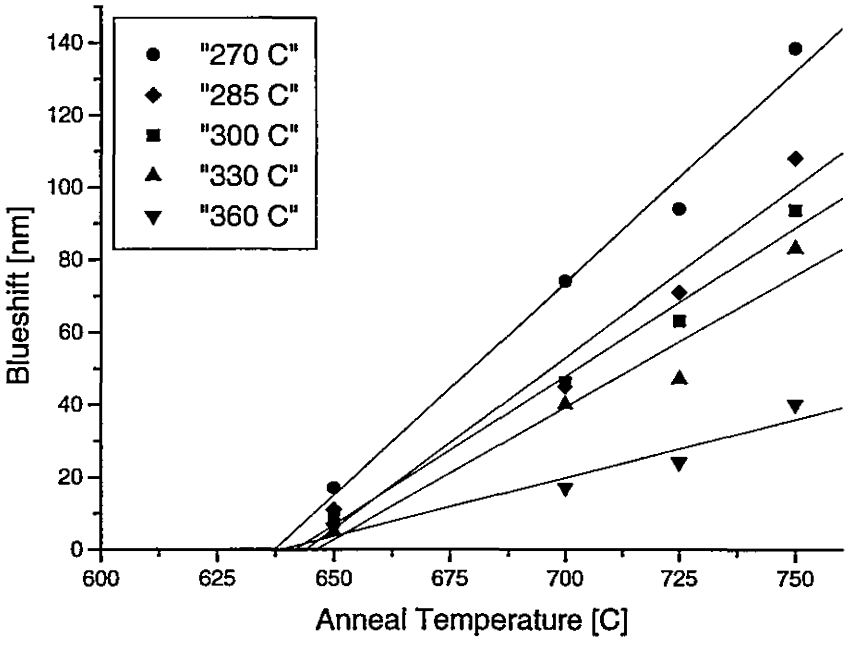

Figure 6.2 The net blueshift caused by the LT-InP cap layer as a function of anneal temperature and shown with respect to the growth temperature of the LT-InP cap.

Figure 6.2 presents the net blueshift as a function of anneal temperature for various samples taken from Figure 6.1. The thermal blueshift, exhibited by sample 3529, is assumed to be an independent, additive process and was subtracted to isolate the rate of change of intermixing caused by the LT-InP cap. Assuming a linear increase, the slopes are presented in Table 2 using a linear regression with $R^2 > 0.97$, where the error is given relative to the line of best fit. However, samples annealed at 750°C appear consistently higher than the expected blueshift, which may be the result of the surface dissociation previously reported in Chapter 5.

Table 2 Calculated Net Rate of Intermixing with Anneal Temperature

Sample Number	LT-InP Growth Temperature [°C]	Rate of Intermixing with Anneal Temperature [nm/°C]
3526	"270"	1.17 ± 0.1
3533	"285"	0.94 ± 0.1
3525	"300"	0.82 ± 0.1
3530	"330"	0.73 ± 0.1
3532	"360"	0.32 ± 0.1

It can be seen that the rate of change in blueshift with anneal temperature increases with decreasing growth temperature. These observations are consistent with previous results [4] for LT-GaAs/AlGaAs structures where the rate of change of blueshift with anneal temperature was not constant relative to the different growth temperatures. The results summarized in Table 2 confirm that the rate of QWI increases with the concentration of defects, more of which are incorporated as the growth temperature is decreased.

From extrapolating the blueshift versus anneal temperature, as shown by the line in Figure 6.2, it is seen that the blueshift becomes zero at an anneal temperature of 642 ± 5°C. This indicates that there is a minimum anneal temperature required to achieve enhanced QWI using LT-InP caps. It is suggested that this temperature provides the necessary thermal energy to dissociate the P_{In} antisite into its P-interstitial and In-vacancy components. Then, since the P-interstitial is highly mobile over the entire anneal range, the QWI proceeds rapidly due to P-interstitial diffusion and the exchange process [13, 14].

To summarise, the term LT-InP caps refers to the non-stoichiometric InP surface layer that is formed by reducing the growth temperature below "400°C". This is consistent with the expectation that the use of excess P_2 flux at growth

temperatures below congruent sublimation (360°C) will result an increase of P_{In} point defects. The onset of the enhanced QWI process at anneal temperatures ~640°C suggests that this is the temperature for dissociation of the P-antisites into a P-interstitial and In-vacancy. It is also seen that the amount of blueshift can be controlled by either the sample anneal temperature or the LT-InP growth temperature.

Effect of Distance to QW's on Intermixing

Figure 6.3 presents the blueshift versus anneal time for full and partial lasers annealed at 700°C and 750°C. Sample 3525 is a partial laser structure with a 100nm thick LT-InP cap grown at 300°C, sample 3541 is a full laser structure with 2μm of undoped InP grown above the active region and terminated with a 100nm thick LT-InP cap grown at 300°C, and sample 3529 is a partial laser structure terminated with a 100nm thick NT-InP cap. This last sample has been included to demonstrate the difference in blueshift between partial laser structures terminated with NT- or LT-InP caps.

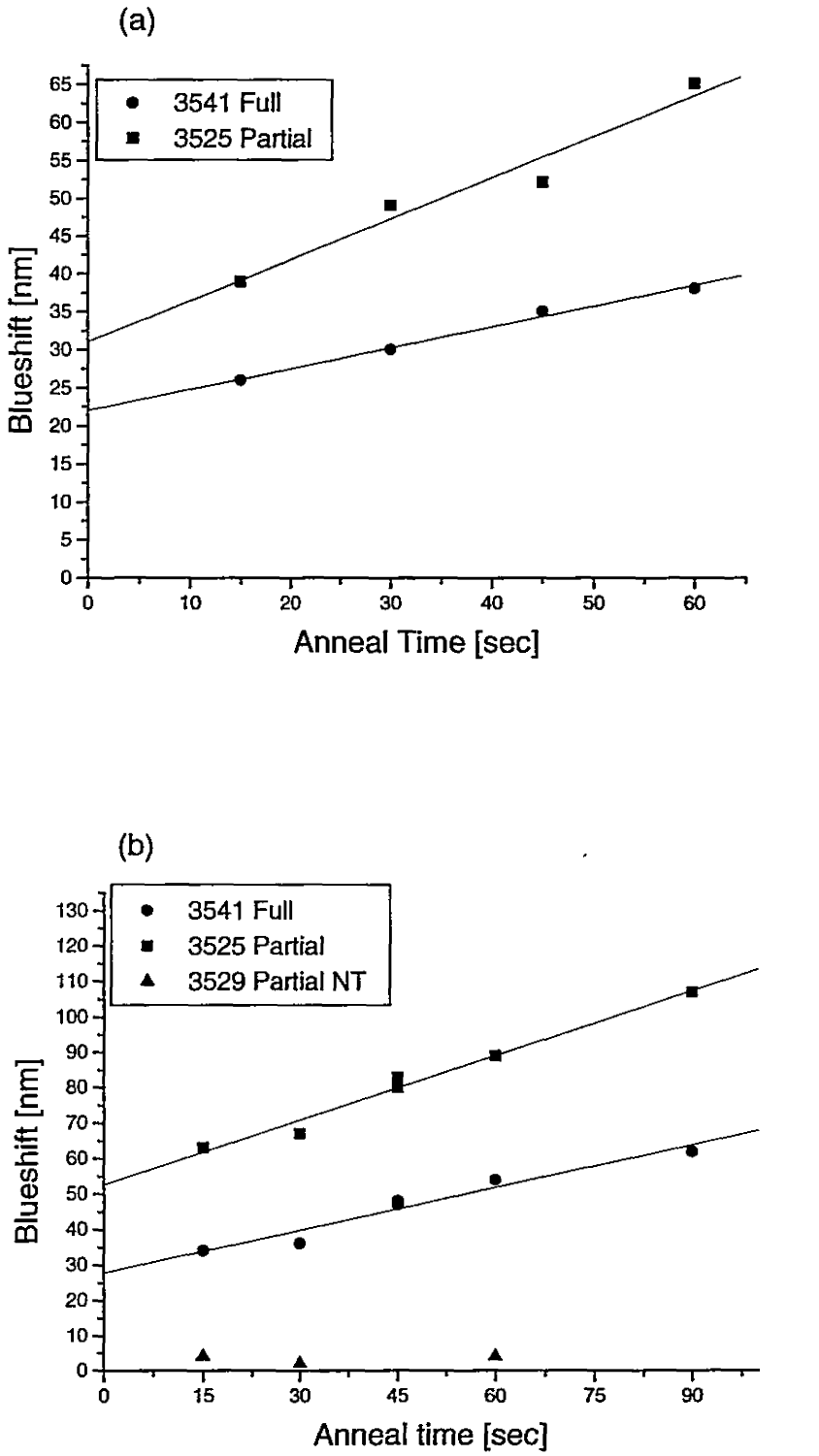

Figure 6.3 Measured blueshift as a function of anneal time for (a) 700°C and (b) 725°C anneals and shown with respect to different sample structures.

A comparison of the partial laser structures terminated with LT-InP or with NT-InP in Figure 6.3 (b) shows that LT-InP is responsible for a much enhanced blueshift compared to the sample terminated with NT-InP. The thermal blueshift of the sample capped with NT-InP agrees well with the results reported in Figure 5.1. Thus the enhanced QWI is a result of mobile defects incorporated in the LT-InP cap during growth, and not from the group V vacancy diffusion observed in Chapter 5, which was caused by surface dissociation at temperatures >690°C.

From Figures 6.3 (a, b) it can be seen that both the full and partial samples terminated with LT-InP exhibit a large blueshift even after anneals as short as 15 sec. This initial blueshift further increases at the higher anneal temperature for both the full and partial laser structures, which is consistent with the results presented in Figure 6.2. It is also seen that the partial laser exhibits a consistently larger blueshift than the full laser for all anneal temperatures and times.

For times >15 sec, if we consider a linear increase in blueshift with time, shown by the lines in Figure 6.3, it is noted that the rate of increase in blueshift with time is greater at the higher anneal temperature. It is also noted that the slopes in Figure 6.3 are consistently greater for the partial laser than for the full laser structure. The reduced blueshift occurring in the full laser structure will result from the additional 2μm of undoped InP above the active region through which the defects from the LT-InP cap must diffuse. This is further evidence that the enhanced QWI is the result of defects originating from the LT-InP cap that

have to diffuse through an extra 2μm of InP in the full laser before reaching the quantum wells.

Effect of LT-InP on Intermixing as a function of Phosphine Flow

During growth by GSMBE, incident group V atoms are incorporated with the group III species on the sample surface such that excess group V atoms are desorbed, yielding a stoichiometric material. Normal growth temperature for the GSMBE system at McMaster is 470°C (or "517°C" as read by the thermocouple). This temperature is considerably greater than congruent sublimation, therefore the growth rate is determined by the total group III flux, and stoichiometry is maintained by a large chemical potential in the form of group V overpressure during growth [57].

InP grown at low temperatures, below the congruent sublimation temperature, has been shown to be n-type with a donor concentration of $2x10^{18}$ cm^{-3} [36]. Subsequent studies [58, 59] have further shown that LT-InP epitaxial layers grown with large V:III flux ratios result in a greater concentration of donors, which have been correlated to the P_{In}^{+} defects [37].

A previous analysis [36] on LT-InP epitaxial layers grown by GSMBE at McMaster found that the minimum phosphine flow required to maintain good crystal quality is between 1.5 and 2sccm. The samples used in this study are partial laser structures terminated with either 100nm of LT-InP grown at "300°C" or 100nm of NT-InP. Samples are grown with a phosphine flow that was varied within the range of 2.0 to 5.75sccm, the largest value attainable with McMaster's GSMBE system. All samples were subsequently annealed for 30 sec with InP

proximity caps at temperatures ranging between 650-750°C and the resulting blueshift is shown in Figure 6.4. We assume that the P_2 flux that is used in the growth is directly proportional to the phosphine flow into the cracker cell. This assumes that the cracker cell efficiency is independent of the pressure within the cracking region.

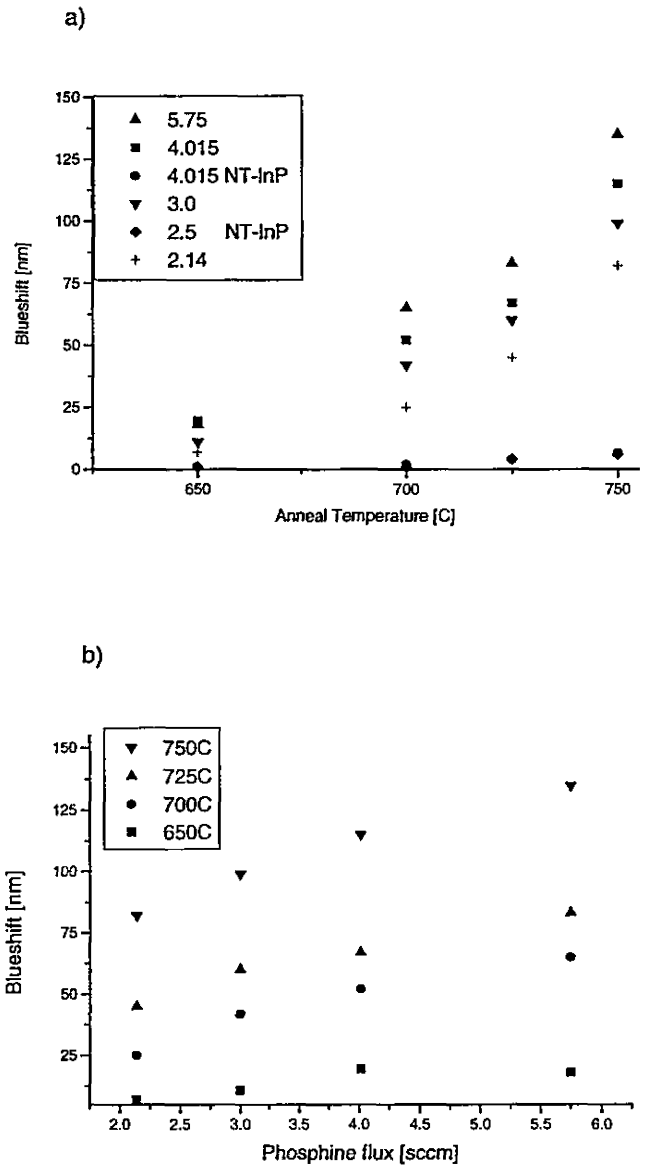

Figure 6.4 Measured blueshift for a 30 sec anneal (a) as a function of anneal temperature and shown with respect to the growth conditions of the InP cap and (b) as a function of the phosphine flow [sccm] used to grow the LT-InP cap and shown with respect to anneal temperature.

Two samples with NT-InP caps were also grown with different phosphine flows (4.0 and 2.5 sccm) at normal growth temperature. Since the QWI is the

same for both NT-InP samples shown in Figure 6.4 (a) we can infer that no defects are incorporated for both phosphine flow rates. However, samples with LT-InP caps can be seen in Figures 6.4 (a, b) to exhibit increasing blueshift with anneal temperature, and also with increasing phosphine flow.

For low temperature growths (<360°C) the concentration of P related defects incorporated in the LT-InP cap will increase with the phosphine flow. This is consistent with previous results [58, 59] which showed that the incorporation of P_{In} antisites increases with the P_2 flux used during growth. The results in Figure 6.4 are further evidence of a direct correlation between the mobile defects that enhance QWI and the excess phosphorus in the LT-InP cap, which is expected to be incorporated as P_{In}.

It was previously observed that there is a minimum anneal temperature of 642 ± 5°C required to observe QWI. Similarly, in Figure 6.4 (a) extrapolating the data back to zero blueshift yields a temperature of ~644°C, below which no QWI occurs. These results confirm that at a temperature of >640°C the sample has sufficient thermal energy for the P_{In} antisites to dissociate producing a P-interstitial that subsequently diffuses rapidly through the active region to enhance QWI.

Evidence of surface roughness in the cap layer

It can be seen in Figure 6.1 that sample 3526 exhibits the largest blueshift at all anneal temperatures. The LT-InP cap layer was grown at "270°C" with excess P_2 flux and upon removal from the growth chamber the sample clearly showed evidence of surface roughness by its lack of reflectivity. This poor surface morphology is expected to result from the low surface mobility of the depositing In atoms and will result in a highly defected layer. Extended defects may also arise from the condensation of various point defects. It has previously been shown [39] that LT-InP layers are polycrystalline at growth temperatures <265°C and eventually become amorphous at sufficiently low growth temperatures. Thus, the application of LT-InP films for inducing QWI is probably limited to the situation where good crystalline films can be grown. A high concentration of large crystal defects may actually act to trap the migrating defects used to cause the intermixing.

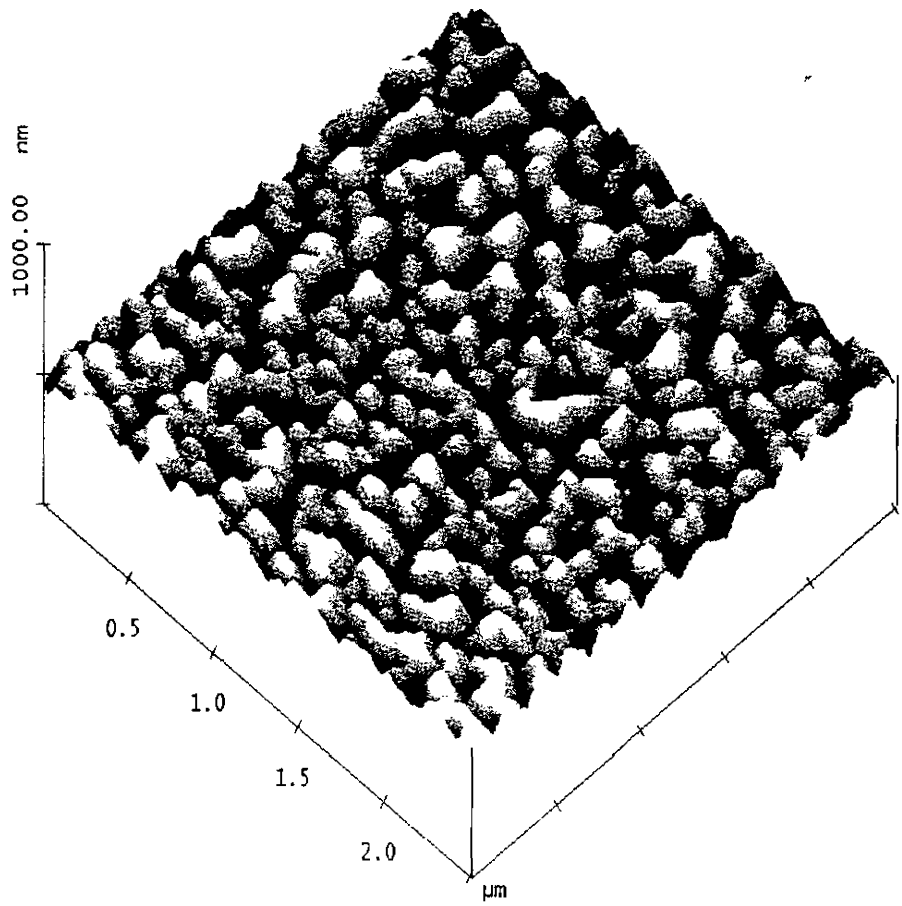

Figure 6.5 Results from AFM analysis on the rough surface of sample 3526 terminated with LT-InP grown at 270°C.

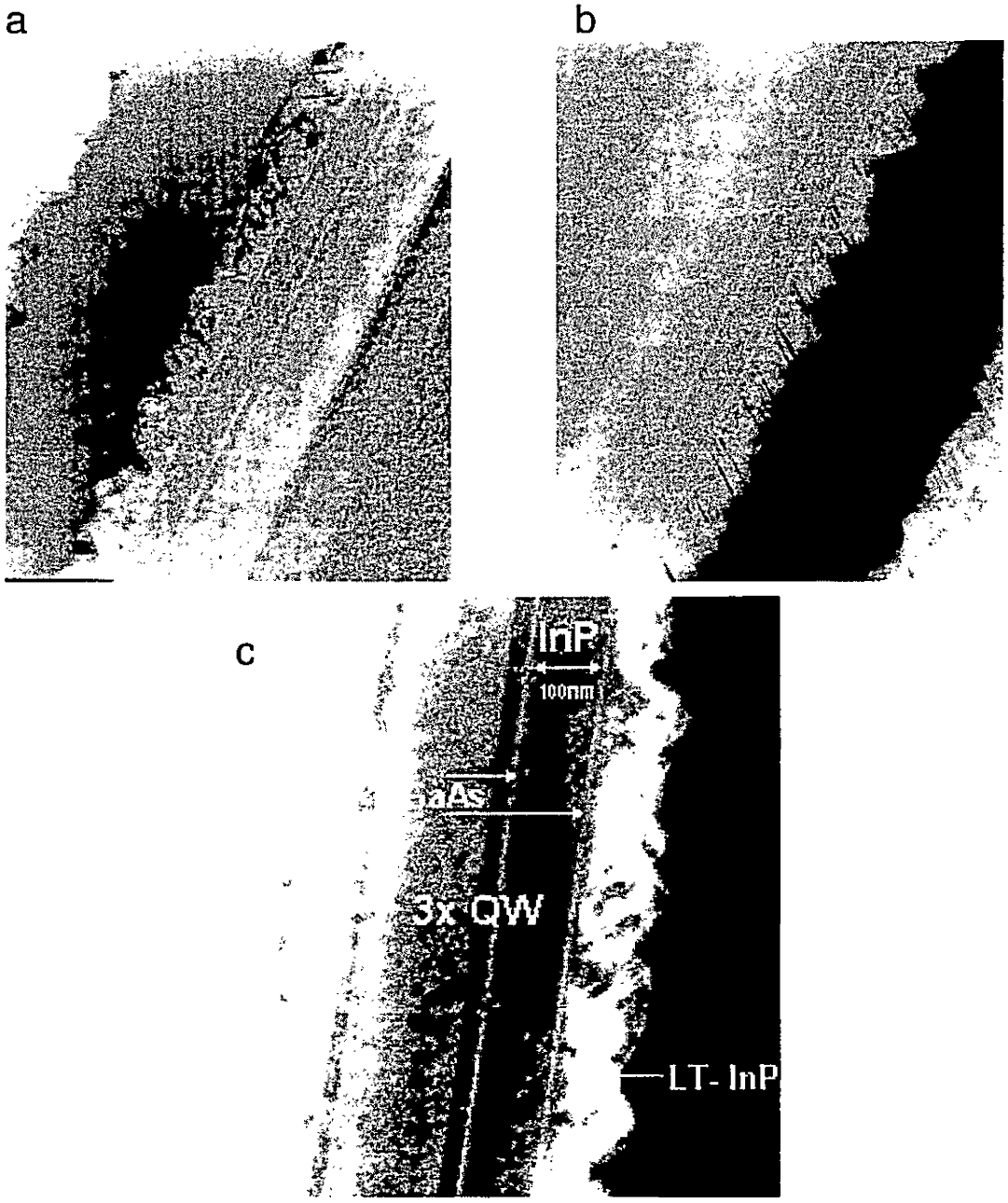

Figure 6.6 Results from TEM analysis of sample 3526 showing surface defects along the (111) planes of the fcc lattice structure. (a) shows the defect planes using low magnification, (b) clearly shows one orientation of the defect planes and (c) reveals the partial laser structure.

Atomic force microscopy (AFM) was performed on a sample grown at "270°C". The result is shown in Figure 6.5. A cross-sectional analysis showed surface roughness in the form of uneven peaks with a typical peak to valley height of 122 ± 6nm and peak to peak separation of 146 ± 8nm. This differs from the other LT-InP growths included in this report which were featureless and mirror-like. This as grown partial laser structure was further characterised using cross-sectional transmission electron microscopy (TEM). The sample was tilted by 5° to form a clear diffraction pattern of the fcc crystal lattice with respect to the [0ll] direction of the electron beam. Measurements of the structure coincide with the schematic presented in Figure 3.3. The three QW's that make up the active region of the laser structure are identified in Figure 6.6 (c), where the direction of growth is from left to right. The thin white lines have been identified as the 5nm thick InGaAs etch stops, which are used for selective chemical wet etch of the upper layers, and the surrounding 25nm and 100nm of undoped InP appear dark grey in colour. Finally, the LT-InP surface layer of the sample is marked by roughness in the form of uneven peaks.

In Figures 6.6 (a, b) the sloped dark lines seen in the LT-InP layer are dislocations along the (111) direction. These crystal defects, possibly the result of strain [24, 26, 36] due to a large incorporation of P_{In} antisites, are initiated at the InGaAs/LT-InP growth interface. If these defects were to propagate through the device active region after annealing they would create scattering centres that can decrease the device performance such as the current threshold and its emission characteristics [60].

Surface Protection During RTA Using Additional Coatings of SOG

The results of Figure 6.7 include sample 3200, which is a partial laser terminated with a LT-InP cap grown at "300°C". In addition to the InP proximity caps used during annealing, "LT-InP, SOG" samples have a coating of commercial (1:1:1) spin on glass (SOG) deposited at room temperature at 4000rpm for 30 sec on top of the LT-InP cap layer. A dielectric layer is often deposited during device processing and, if present during high temperature annealing, it is necessary that it does not further induce intermixing. "Cap Removed" samples had the LT-InP cap layer removed by chemical wet etch to observe the thermal blueshift of the underlying semiconductor material. Samples were annealed for 30 sec and the maximum anneal temperature was limited to 750°C to minimise surface degradation of the sample.

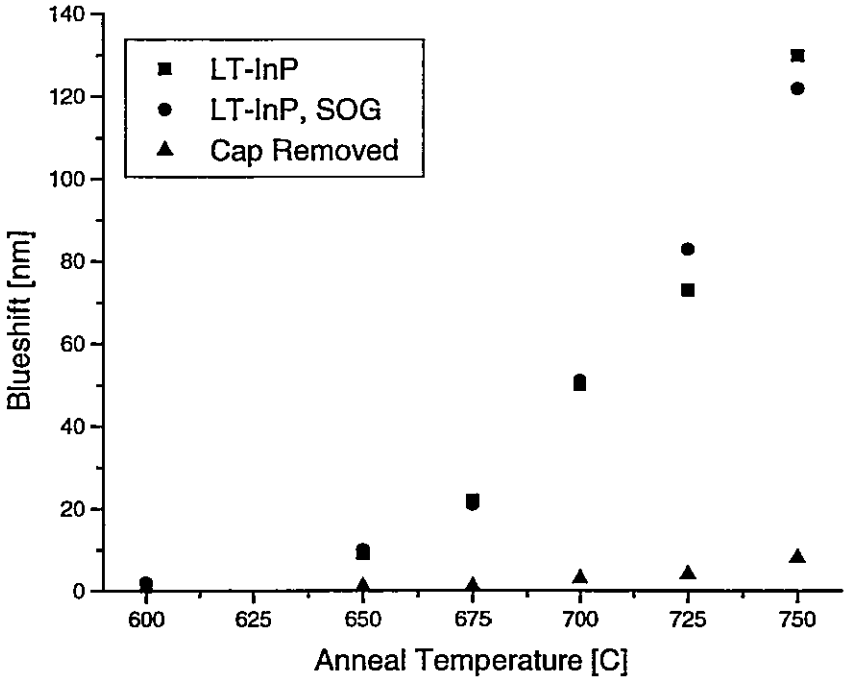

Figure 6.7 Measured blueshift as a function of anneal temperature for a 30 sec anneal.

The partial laser sample in Figure 6.7 with the LT-InP cap removed exhibits <10nm of blueshift after a 30 sec anneal at temperatures up to 750°C. This is consistent with the thermal blueshift that was observed in Figure 5.1. Both samples with LT-InP caps in Figure 6.7 exhibit essentially identical enhanced blueshifts with anneal temperature. This observation that a coating of SOG does not affect the blueshift has previously been observed [16], and is confirmed here.

All samples were annealed with InP proximity caps; however, at 750°C samples without a coating of SOG appeared to exhibit some surface damage. Under a microscope In droplets were seen on the surface indicating that P_2 evaporation had occurred. However, no evidence of surface dissociation has

been observed for annealed samples with the SOG coating removed by chemical wet etch [61]. These results suggest that the deposition of SOG may be used to prevent surface damage due to evaporation at high temperatures.

Conclusions

Samples terminated with LT-InP undergo QWI upon anneal. The degree of intermixing can be controlled by the anneal temperature-time profile and also by the growth conditions of the cap layer. In particular, reducing the temperature or increasing the P_2 flux during growth of the LT-InP cap layer will result in an increase of incorporated defects. This intermixing, as indicated by the blueshift of the PL peak energy, is not observed for InP layers grown >360°C, which coincides with the temperature of congruent sublimation for InP. However, at sufficiently low temperatures (<"270°C") the epitaxial layer was found to be heavily faulted with crystal defects, indicating that the incorporation of excess P leads to polycrystalline growth. Furthermore, this enhanced QWI is not observed for samples where the LT-InP cap has been removed by chemical wet etch before annealing. These results clearly indicate that mobile defects are present in the LT-InP cap layer, which diffuse to enhance QWI.

It was shown that the intermixing increases steadily with increasing anneal time and for anneal temperatures >640°C. These results suggest that a large concentration of defects are present in the LT-InP cap layer. Furthermore, the defects have a high mobility, as indicated by the blueshift of the full laser structure, which exhibited a large blueshift within <15sec of annealing at 700°C. It has been postulated that the defects are associated with P_{In} antisites, which

have previously been shown to be incorporated with increasing concentration in LT-InP as the growth temperature is decreased and also with increasing P_2 flow. It is proposed that there is sufficient thermal energy at anneal temperatures >640°C for the antisites in the LT-InP cap to dissociate. The resulting P interstitial has a high mobility and subsequently diffuses rapidly through the active region to enhance QWI.

Chapter 7

Summary of Work

Conclusions Regarding the Study of Thermal Blueshift

A blueshift in the PL emission from the QW's is indicative of intermixing between the wells and barriers in the active region. High quality crystals have small interdiffusion coefficients of the host species [3, 47]; thus the thermal blueshift refers to the intermixing that occurs during annealing as a result of the diffusion of grown-in defects incorporated in the sample. There appear to be several processes contributing towards this observed thermal blueshift.

(1) Full laser structures grown on purchased n-type substrates with Be-doped upper cladding layers exhibit a large blueshift (>25nm) that occurs within <8 sec when the samples are annealed at 700°C. However, similar structures with undoped upper cladding layers and partial laser structures do not exhibit this large blueshift. It should also be noted that a reduction in the growth temperature of the active region of the full laser structures by up to 40°C does not alter the thermal response of the material. This large blueshift is essentially independent of anneal temperature at short anneal times (<8 sec), which suggests that it is related to the fixed Be doping in the upper cladding layers. It was speculated that a grown-in defect complex in the Be-doped cladding layer dissociates at anneal

temperatures above the growth temperature but below 700°C, which produces a highly mobile, intrinsic defect that is likely to be a P_i.

A mirrored doping structure, grown on a p-type substrate (Zn-doped) with Si-doped upper cladding layers, exhibited a consistently larger blueshift the structure grown on an n-type substrate (S-doped) under the same annealing conditions. This enhanced blueshift may also be the result of a grown-in defect complex present in the Si-doped upper cladding layer, or possibly additional defects present in the purchased Zn-doped substrate.

(2) The partial laser structures also exhibit a rapid increase in blueshift at short anneal times (<8sec) but for temperatures ≥750°C. This blueshift was shown to be independent of the surface layer (InGaAs or InP) of the sample. It has been proposed that possibly another grown-in defect complex, originating from the active region and/or surrounding doped guiding layers, dissociates at anneal temperatures ≥750°C to produce a fast diffusing intrinsic defect that contributes to the enhanced QWI.

(3) It was also shown that a steady increase in blueshift with anneal temperatures ≥750°C is exhibited for both full and partial laser structures grown without LT-InP caps. Upon removal from the furnace these samples were found to have In-rich surfaces which appeared frosted. This process of QWI has an onset at ~690°C, as seen from the thermal response of the partial laser structures, and dominates in both full and partial laser structures for 60 sec anneals at temperatures ≥750°C. This thermal blueshift may be the combination of the dissociation of a defect complex and also group V vacancy diffusion

originating from the desorption of group V species from the sample surface. These results indicate that the use of proximity caps may not be adequate protection of the sample surface for prolonged anneals at temperatures >750°C. However, an additional coating of SOG does not further enhance QWI and could possibly be used to preserve the sample surface at high temperatures.

Conclusions Regarding the Study of QWI Using LT-InP

The blueshift exhibited by samples with undoped upper guiding and cladding layers, and terminated with InP grown at temperatures greater than the congruent sublimation temperature of InP (360°C) is similar to the thermal blueshift previously observed for samples grown at normal temperatures. Similar characteristics were also observed for both full and partial undoped laser structures with the LT-InP cap removed by chemical wet etch prior to annealing. These results indicate that the growth of LT-InP surface layers does not increase the concentration of defects in the underlying semiconductor material. Furthermore, the blueshift of laser structures capped with LT-InP is consistently larger for partial laser structures than for full lasers due to the 2μm of undoped InP grown above the active region of the full lasers through which any defects in the layers at the top of the structure must diffuse. These results suggest that samples with InP caps grown below congruent sublimation temperature contain defects that are incorporated in the cap layer as a result of non-stoichiometric growth and diffuse to enhance QWI.

It was further shown that the blueshift of partial laser structures terminated with LT-InP steadily increases with decreasing growth temperature of the cap layer and also increases linearly with increasing phosphine flow. These results were used to show that the rate of intermixing increases with the concentration of defects incorporated in the LT-InP cap. Previous studies have shown that the concentration of P_{In} antisites in LT-InP increases with decreasing growth temperature [24, 37, 39] and also with increasing P_2 flux [58, 59]. Furthermore, the concentration of P_{In}^+ is sufficiently large that the n-type material, formed by the autoionization of P_{In}^+ remains n-type even for Be-doping (p-type) > $10^{18}cm^{-3}$ [26, 37, 40]. Therefore, it is postulated that the large concentration of defects incorporated in the LT-InP cap layer are associated with P_{In} antisites and this concentration is sufficiently large to obtain a blueshift >100nm in the measured PL peak energy upon annealing.

It has been shown [39] that at growth temperatures <265°C the LT-InP material becomes poly-crystalline. This is consistent with the growth of sample 3526, which was terminated with a LT-InP cap grown at "270°C" with excess phosphine flow. The LT-InP layer was found to have a rough surface and contained dislocations in the (III) direction. These results suggest that a large concentration of excess P was incorporated as P_{In} antisites, which resulted in a strained layer. This indicates that the growth temperature used to incorporate excess P related defects in a single crystal epitaxial layer of LT-InP must be maintained above "270°C".

Finally, it was shown that the blueshift of samples terminated with LT-InP increases steadily with anneal time and also with anneal temperatures greater than ~640°C. Furthermore, a large blueshift was observed within <15 sec when samples were annealed at 700°C, which suggests that the defects contributing to the enhanced QWI are highly mobile. Therefore, it is proposed that at anneal temperatures >640°C there is sufficient thermal energy for the P_{In} antisite to dissociate, resulting in a P interstitial which diffuses rapidly through the active region due to its high mobility [43] and causes the enhanced QWI.

Potential Applications for Device Processing Using LT-InP

It has been demonstrated that the as grown wavelength of a laser structure can be altered post-growth using QWI. Previous studies [10, 16, 49] have shown that the area-selectivity using dielectric encapsulation and ion implantation is sufficiently precise to form integrated devices. Similarly, an integrated laser/waveguide could be processed using LT-InP techniques.

Ideally, in order to produce a photonic integrated circuit it is desirable that the wavelength of the laser section remains unchanged during the thermal treatment necessary to induce QWI. This requires a technique involving low temperature processing. As such, the LT-InP method has advantages over other reported methods. In the previous sections we have shown that very significant blueshifts can be obtained for 30 sec anneals at temperatures as low as 700°C (see Figure 6.1 where for LT-InP grown at 270°C a blueshift of 80nm is obtained whilst the thermal only component is only 2-3nm). We have shown that the regions capped with LT-InP will undergo enhanced QWI, resulting in a larger bandgap, whereas the regions where the LT-InP has been selectively etched will exhibit negligible blueshift. The intermixed regions below the LT-InP would therefore function as a passive waveguide for the light emitted from the active laser, which would be fabricated in the regions where the LT-InP had been removed by chemical etching prior to the RTA treatment. The result would be a waveguide integrated on a single substrate with a laser that emits approximately at the as grown wavelength. A sketch of an integrated waveguide/laser device is

shown in Figure 7.1. A comparison of the QWI process applied to full and partial laser structures suggests that the best results would be obtained using the QWI step at the partial laser stage in the growth. After the anneal and removal of the remaining LT-InP, regrowth of the device would be completed for subsequent fabrication of the ridge features of the ridge waveguide laser structure.

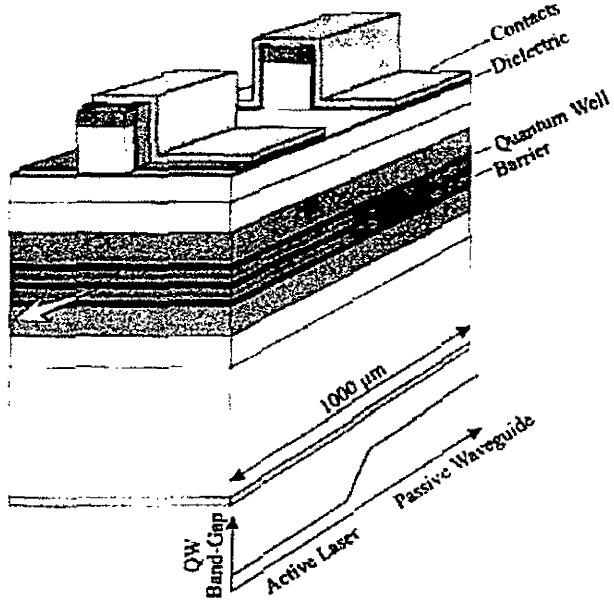

Figure 7.1 Diagram of a laser structure that has undergone selective area QWI prior to device processing[1].

The cap layer of LT-InP is patterned using photolithography techniques and then annealed to induce the spatially defined QWI. Post-anneal, the patterned LT-InP must be completely removed by chemical wet etch to ensure a planar surface upon which regrowth and subsequent fabrication will occur. The

[1] adapted from [16]

primary challenge to process such an integrated device would be the use of alignment markings such that the ridge waveguide is correctly aligned above the previously patterned layer of LT-InP.

A partial laser structure was chosen for this study to facilitate measurements of the blueshift. A quarter wafer was patterned using photo-lithography techniques to create 1.5mm stripes of LT-InP on the sample surface. Following a 30 sec anneal at 725°C, the PL measurements of regions with LT-InP exhibited a blueshift of 68 ± 5nm and the regions where the LT-InP cap had been chemically etched measured <2nm of blueshift. This magnitude is consistent with the results presented in Figure 6.1, indicating that the blueshift can be controlled using the anneal temperatures/times presented in this report. However, further investigation is required to establish the area selectivity of this process of intermixing since the boundaries of the laser/waveguide device may extend beyond the edge regions of the LT-InP stripes if the defects diffuse laterally as well as downward.

Successful fabrication of integrated laser/modulator devices over selectively intermixed regions has been previously demonstrated in literature [49, 62]. However, one problem that needs to be resolved for the completed process of partial growth – QWI – etch and MBE regrowth is the observation that after the regrowth step, surface defects have been found to be present above the intermixed regions [16]. Work needs to be done to overcome this problem and possible experiments should explore different surface preparation processes for the regrowth step.

Suggestions for Future Work

This report suggests several possibilities for subsequent investigations. It was shown that doped, full laser structures exhibit a rapid increase in blueshift at the onset of anneal. Doping is an integral part of the design of semiconductor diode lasers to provide recombination in the active region through control of the current flow through the device [2]. A systematic study of Be and Si doping within the structure is required to correlate the effect of doping on the observed blueshift and possibly identify the mobile defects which enhance QWI. Also, the diffused defects may increase the free carrier absorption in the intrinsic active region, which subsequently becomes the core of the integrated waveguide. Therefore, a study on optical losses of light propagating through the intermixed regions of the sample will determine its usefulness as a waveguide in the fabrication of integrated devices.

Appendix

Glossary of Abbreviations

AFM	Atomic Force Microscopy
As_{Ga}	Arsenic anti-sites
CW	Continuous Wave
DI	De-Ionised water
EPR	Electron Paramagnetic Resonance
GSMBE	Gas Source Molecular Beam Epitaxy
IFVD	Impurity Free Vacancy Disordering
IID	Impurity Induced Disordering
In_i	Indium interstitials
In_P	Indium anti-sites
LID	Laser Induced Disordering
LT-GaAs	Low Temperature grown GaAs
LT-InP	Low Temperature grown InP
MBE	Molecular Beam Epitaxy
MOCVD	Metal-Organic Chemical Vapour Deposition
MOMBE	Metal-Organic Molecular Beam Epitaxy
NT-InP	Normal Temperature grown InP
ODMR	Optically Detected Magnetic Resonance
OEICS	Optoelectronic Integrated Circuits
PAID	Photoabsorption Induced Disordering
PECVD	Plasma Enhanced Chemical Vapour Deposition
PICS	Photonic Integrated Circuits
P_i	Phosphorus interstitials
P_{In}	Phosphorus anti-sites
PL	Photoluminescence
RTA	Rapid Thermal Anneal
QW	Quantum Well
QWI	Quantum Well Intermixing
SIMS	Secondary Ion Mass Spectroscopy
SOG	Spin On Glass
V_{Ga}	Gallium Vacancies
V_P	Phosphorus Vacancies

Works Cited

[1] S. E. Miller, Bell System Technical Journal 48 (1969) 2059-2069

[2] B.G. Streetman, Solid State Electronic Devices. 4th ed. USA: Prentice Hall, 1995.

[3] J. H. Marsh, Semiconductor Science Technology 8 (1993) 1136-1155

[4] W. Feng, F. Chen, W.Q. Cheng, Q. Huang & J.M. Zhou, Applied Physics Letters 71 (1997) 1676-1678

[5] K. Nakashima, Y. Kawaguchi, Y. Kawamura, H. Asahi & Y. Imamura, Japanese Journal of Applied Physics 26 (1987) L1620-1622

[6] J.S. Tsang, C.P Lee, S.H. Lee, K.L. Tsai, & H.R. Chen, Journal of Applied Physics 77 (1995) 4302-4306

[7] S.A. Bradshaw, J.H. Marsh & R.W. Glew, 4th Inernational Conference on InP & Related Materials. NewYork: IEEE, 1992. 604-607

[8] P. Jessop, Engineering Physics 704 "Optoelectronics". McMaster University, 2001

[9] S.Charbonneau, P.J. Pool, P.G. Piva, G.C. Aers, E.S. Koteles, M. Fallahi, J.J. He, J.P. McMaffrey, M. Muchanana, M. Dion, R.D. Goldberg & I.V. Mitchell, Journal of Applied Physics 78 (1995) 3697-3705

[10] J.P. Noel, D. Melville, T. Jones, F.R. Shepherd, C.J. Miner, N. Puetx, K. Fox, P.J. Poole, Y. Feng, E.S. Koteles, S. Charboneau, R.D. Goldberg & I.V. Mitchell, Applied Physics Letters 69 (1996) 3516-3518

[11] E.V.K. Rao, A. Hamoudi, Ph. Krauz, M. Juhel & H. Thibierge, Applied Physics Letters 66 (1995) 472-474

[12] J.E. Haysom, G.C. Aers, S. Raymond & P. Poole, Journal of Applied Physics 88 (2000) 3090-3092

[13] J.E. Haysom, P.J. Poole, R.L. Williams, S. Raymond, G.C. Aers, Solid State Communications 116 (2000) 187-190

[14] A.S.W. Lee, D.A. Thompson, J. Bursik, B.J. Robinson & G.C. Weatherly, Applied Physics Letters 78 (2001) 3199-3201

[15] J.H. Marsh and A.C. Bryce, Materials Science & Engineering B28 (1994) 272-278

[16] J.F. Hazell, Ph.D Thesis, McMaster University, 2000

[17] A. Ramdane, P. Krauz, E.V.K. Rao, A. Hamoudi, A. Ougazzaden, D. Robein, A. Gloukhian & M. Carré, IEEE Photonics Technology Letters 7 (1995) 1016-1018

[18] N. Cao, B.B. Elenkrig, J.G. Simmons, D.A. Thompson, N. Puetz, Applied Physics Letters 70 (1997) 3419-3421

[19] B.L. Weiss, Y. Chan, W.C. Shiu, E. H. Li, Journal of Applied Physics 88 (2000) 3418-3425

[20] H. Chen, R.M. Feenstra, P.G. Piva, R.D. Goldberg, I.V. Mitchell, G.C. Aers, P.J. Poole & S. Charbonneau, Applied Physics Letters 75 (1999) 79-81

[21] L. Fu, P.N.K. Deenapanray, H.H. Tan, C. Jagadish, L.V. Dao & M. Gal, Applied Physics Letters 76 (2000) 837-839

[22] S. Balasubramanian, D.D. Nolte & M.R. Melloch, Journal of Applied Physics 88 (2000) 4576-4581

[23] X.F. Liu, B.C. Qiu, M.L. Ke, A.C. Bryce & J.H. Marsh, IEEE Photonics Technology Letters 12 (2000) 1141-1143

[24] D.P. Docter, J.P Ibbetson, Y. Gao, U.K. Mishra, T. Liu & D.E. Grider, Journal of Electronic Materials 27 (1998) 479-483

[25] K. Xie, C.R. Wie & G.W. Wicks, Materials Research Society Symposium Proceedings 241 (1992) 265-267

[26] H.J. von Bardeleben, Y.Q. Jia, J.P Hirtz, J.C. Garcia, M.O. Manasreh, C.E. Stutz & K.R. Evans, Materials Research Society Symposium Proceedings 241 (1992) 69-74

[27] G.N. Maracas, K.T. Shiralagi, R.A. Puechner, F. Yu, K.T. Choi, J.S. Bow, R. Ramamurti, M.J. Kim & R.W. Carpenter Materials Research Society Symposium Proceedings 241 (1992) 271-276

[28] P. Hautojärvi, J. Mäkinen, S. Palko , K. Saarinen, C. Corbel & L. Liszkay, Materials Science & Engineering B22 (1993) 16-22

[29] G.N. Maracas, K. Shiralagi, R. Ramamurti & R.W. Carpenter, Journal of Electronic Material 22 (1993) 1375-1381

[30] M.R. Melloch, J.M. Woodall, E.S. Harmon, N. Otsuka, F.H. Pollak, D.D. Nolte, R.M. Feenstra & M.A. Lutz, Annual Review of Materials Science 25 (1995) 547-600

[31] J.S. Tsang, C.P. Lee, J.C. Fan, K.L. Tsai & H.R. Chen, Journal of Vacuum Science Technology B13 (1995) 1536-1538

[32] D.G. Deppe & N. Holonyak Jr., Journal of Applied Physics 64 (1988) R93-R111

[33] J.S. Tsang, C.P. Lee, S.H. Lee, K.L. Tsai, C.M. Tsai & J.C. Fan, Journal of Applied Physics 79 (1996) 664-670

[34] J.Ch. Garcia, J.P. Hirtz, P. Maurel, H.J. von Bardeleben & J.C. Bourgoin, Materials Research Society Symposium Proceedings 241 (1992) 277-282

[35] B.W. Liang, Y. He & C.W. Tu, Materials Research Society Symposium Proceedings 241 (1992) 283-288

[36] D.B. Mitchell, Ph.D Thesis, McMaster University, 1995

[37] P.Dreszer, W.M. Chen, K. Seendripu, J.A. Wolk, W. Walukiewicz, B.W. Lian, C.W. Tu & E.R. Webber, Physical Review B47 (1993) 4111-4114

[38] P. Dreszer, W.M. Chen, D. Wasik, R. Leon, W. Walukiewicz, B.W. Liang, C.W. Tu & E.R. Weber, Journal of Electronic Materials 22 (1993) 1487-1490

[39] W.M. Chen, I.A. Buyanova & C.W. Tu, Materials Sci & Eng B75 (2000) 103-109.

[40] B.W. Liang, P.Z. Lee, D.W. Shih & C.U. Tu, Applied Physics Letters 60 (1992) 2104-2106

[41] T.M. Schmidt, R.H. Miwa, A. Fazzio & R. Mota, Physical Review B60 (1999) 16475-16478

[42] A.S.W. Lee, D.A. Thompson & B.J. Robinson, Semiconductor Science Technology 15 (2000) L41-L43

[43] K. Karsten & P. Ehrhart, Physical Review B51 (1995) 10508-10519

[44] S. Komiya, T. Tanahshi & I. Umebu, Japanese Journal of Applied Physics 24 (1985) 1053-1055

[45] Mini-Pulse System Manual. AG Associates. Document #82071-0100, 1991

[46] P. Mascher & D.A. Thompson, Engineering Physics 727 "Thin Film Growth, Deposition and Characterization", McMaster University 2001

[47] B. Goldstein, Physical Review 121 (1961) 1305-1311

[48] R.E. Mallard, N.J. Long, E.J. Thrush, K. Scarrott, A.G. Norman & G.R. Brooker, Journal of Applied Physics 73 (1993) 4297-4303

[49] A. Hamoudi, E.V.K. Rao, Ph. Krauz, A. Ramdane, A. Ougazzaden, D. Robein & H. Thibierge, Journal of Applied Physics 78 (1995) 5638-5641

[50] H. Pinkney, D.A. Thompson, B.J. Robinson, P.J. Simpson, U. Myler & R. Streater, 11th International Conference on InP and Related Materials. NY:IEEE, 1999. p143-146

[51] Private Communication with Dr. D.A. Thompson on October 4, 2002 regarding unpublished results on impurities

[52] J.H. Marsh, S.A. Bradshaw, A.C. Bryce, R. Gwilliam & R.W. Glew, Journal of Electronic Materials 20 (1991) 973-8

[53] G.J. van Gurp, W.M. van de Wijgert, G.M. Fontijn and P.J.A. Thijs Journal of Applied Physics 67 (1990) 2919-2926

[54] Private Communication with Dr. D.A. Thompson regarding unpublished results on sample doping

[55] R.W. Glew, A.T.R. Briggs, P.D. Greene & E.M. Allen. Proceedings 4th International Conference on InP and Related Materials. New York: IEEE, 1992. p604-607

[56] P.W. Yu, B.W. Liang & C.W. Tu, Applied Physics Letters 61 (1992) 2443-2445

[57] K. Ploog 3D Crystals: Growth, Properties & Applications. Berlin: Springer-Verlag, 1980.

[58] S.F. Yoon, H.Q. Zheng, P.H. Zhang, K.W. Mah & G.I. Ng, Thin Solid Films 326 (1998) 233-237

[59] S.F. Yoon, H.Q. Zheng, P.H. Zhang, K.W. Mah, G.I. Ng, Japanese Journal of Applied Physics 38 (1999) 981-984

[60] D.T. Cassidy, Engineering Physics 723 "Semiconductor Diode Lasers", McMaster University, Fall 2001

[61] Private Communication with A.S.W. Lee on October 25, 2002 regarding annealed samples coated with SOG

[62] G. Letal, Ph.D Thesis, McMaster University, 2000